

RUNNING HEAD: Networks across human menstrual cycle

Functional reorganization of brain networks across the human menstrual cycle

Laura Pritschet^{1*}, Tyler Santander^{1*}, Caitlin M. Taylor¹, Evan Layher¹, Shuying Yu¹,
Michael B. Miller^{1,2,3}, Scott T. Grafton^{1,2}, & Emily G. Jacobs^{1,3}

¹Department of Psychological & Brain Sciences, University of California, Santa Barbara, Santa Barbara, CA

² Institute for Collaborative Biotechnologies, University of California, Santa Barbara, Santa Barbara, CA

³Neuroscience Research Institute, University of California, Santa Barbara, Santa Barbara, CA

* Authors contributed equally to this work.

Correspondence:

Emily G. Jacobs
Department of Psychological & Brain Sciences
University of California, Santa Barbara
Santa Barbara, CA 93106
emily.jacobs@psych.ucsb.edu

Key Words: sex hormones | estrogen | progesterone | functional connectivity | resting-state

Highlights

- Intrinsic fluctuations in sex hormones shape the brain's functional architecture.
- Estradiol facilitates tighter coherence within whole-brain functional networks.
- Progesterone has the opposite, reductive effect.
- Ovulation (via estradiol) modulates variation in topological network states.
- Effects are pronounced in network hubs densely populated with estrogen receptors.

Abstract

The brain is an endocrine organ, sensitive to the rhythmic changes in sex hormone production that occurs in most mammalian species. In rodents and nonhuman primates, estrogen and progesterone's impact on the brain is evident across a range of spatiotemporal scales. Yet, the influence of sex hormones on the functional architecture of the human brain is largely unknown. In this dense-sampling, deep phenotyping study, we examine the extent to which endogenous fluctuations in sex hormones alter intrinsic brain networks at rest in a woman who underwent brain imaging and venipuncture for 30 consecutive days. Standardized regression analyses illustrate estrogen and progesterone's widespread associations with functional connectivity. Time-lagged analyses examined the temporal directionality of these relationships and suggest that cortical network dynamics (particularly in the Default Mode and Dorsal Attention Networks, whose hubs are densely populated with estrogen receptors) are preceded—and perhaps driven—by hormonal fluctuations. A similar pattern of associations was observed in a follow-up study one year later. Together, these results reveal the rhythmic nature in which brain networks reorganize across the human menstrual cycle. Neuroimaging studies that densely sample the individual connectome have begun to transform our understanding of the brain's functional organization. As these results indicate, taking endocrine factors into account is critical for fully understanding the intrinsic dynamics of the human brain.

1 Introduction

2 The brain is an endocrine organ whose day-to-day function is intimately tied to the action
3 of neuromodulatory hormones (Frick et al., 2015; Galea et al., 2017; Hara et al., 2015;
4 Woolley and McEwen, 1993). Yet, the study of brain-hormone interactions in human
5 neuroscience has often been woefully myopic in scope: the classical approach of
6 interrogating the brain involves collecting data at a single time point from multiple
7 subjects and averaging across individuals to provide evidence for a
8 hormone-brain-behavior relationship. This cross-sectional approach obscures the rich,
9 rhythmic nature of endogenous hormone production. A promising trend in network
10 neuroscience is to flip the cross-sectional model by tracking small samples of individuals
11 over timescales of weeks, months, or years to provide insight into how biological,
12 behavioral, and state-dependent factors influence intra- and inter-individual variability in
13 the brain's intrinsic network organization (Gordon et al., 2017; Gratton et al., 2018a;
14 Poldrack et al., 2015). Neuroimaging studies that densely sample the individual
15 connectome are beginning to transform our understanding of the dynamics of human
16 brain organization. However, these studies commonly overlook sex steroid hormones as a
17 source of variability—a surprising omission given that sex hormones are powerful
18 neuromodulators that display stable circadian, infradian, and circannual rhythms in
19 nearly all mammalian species. In the present study, we illustrate robust, time-dependent
20 interactions between the sex steroid hormones 17β -estradiol and progesterone during a
21 complete menstrual cycle. A within-subject replication study further confirms the

22 robustness of these effects. These results offer compelling evidence that sex hormones
23 modulate widespread patterns of connectivity in the human brain.

24 Converging evidence from rodent (Frick et al., 2018, 2015; Woolley and McEwen,
25 1993), non-human primate (Hao et al., 2006; Wang et al., 2010), and human neuroimaging
26 studies (Berman et al., 1997; Jacobs and D'Esposito, 2011; Jacobs et al., 2016a,b; Lisofsky
27 et al., 2015; Petersen et al., 2014) has established the widespread influence of 17β -estradiol
28 and progesterone on regions of the mammalian brain that support higher level cognitive
29 functions. Estradiol and progesterone signaling are critical components of cell survival
30 and plasticity, exerting excitatory and inhibitory effects that are evident across multiple
31 spatial and temporal scales (Frick et al., 2018; Galea et al., 2017). The dense expression of
32 estrogen and progesterone receptors (ER; PR) in cortical and subcortical tissue
33 underscores the widespread nature of hormone action. For example, in non-human
34 primates, ~50% of pyramidal neurons in prefrontal cortex (PFC) express ER (Wang et al.,
35 2010) and estradiol regulates dendritic spine proliferation in this region (Hara et al., 2015).
36 Across the rodent estrous cycle (occurring every 4-5 days), fluctuations in estradiol
37 enhance spinogenesis in hippocampal CA1 neurons, while progesterone inhibits this
38 effect (Woolley and McEwen, 1993).

39 During an average human menstrual cycle, occurring every 25-32 days, women
40 experience a ~12-fold increase in estradiol and an ~800-fold increase in progesterone.
41 Despite this striking change in endocrine status, we lack a complete understanding of how
42 the large-scale functional architecture of the human brain responds to rhythmic changes in

43 sex hormone production across the menstrual cycle. Much of our understanding of
44 cycle-dependent changes in brain structure (Sheppard et al., 2019; Woolley and McEwen,
45 1993) and function (Hampson et al., 2014; Kim and Frick, 2017; Warren and Juraska, 1997)
46 comes from rodent studies, since the length of the human menstrual cycle (at least 5×
47 longer than rodents' estrous cycle) presents experimental hurdles that make longitudinal
48 studies challenging. A common solution is to study women a few times throughout their
49 cycle, targeting stages that roughly correspond to peak/trough hormone concentrations.
50 Using this 'sparse-sampling' approach, studies have examined resting-state connectivity
51 in discrete stages of the cycle (De Bondt et al., 2015; Hjelmervik et al., 2014; Lisofsky et al.,
52 2015; Petersen et al., 2014; Syan et al., 2017; Weis et al., 2019); however, some of these
53 findings are undermined by inconsistencies in cycle staging methods, lack of direct
54 hormone assessments, or limitations in functional connectivity methods.

55 In this dense-sampling, deep-phenotyping study, we determined whether day-to-day
56 variation in sex hormone concentrations impacts connectivity states across major intrinsic
57 brain networks. First, we assessed brain-hormone interactions over 30-consecutive days
58 representing a complete menstrual cycle (Study 1). To probe the reliability of these
59 findings, procedures were then repeated over a second 30-day period, providing a
60 within-subject controlled replication (Study 2). Results reveal that intrinsic functional
61 connectivity is linearly dependent on hormonal dynamics across the menstrual cycle at
62 multiple spatiotemporal scales. Estradiol and progesterone were associated with
63 spatially-diffuse changes in connectivity, both at time-synchronous and time-lagged levels

64 of analysis, demonstrating that intrinsic fluctuations in sex hormones—particularly the
65 ovulatory surge in estradiol—may contribute to dynamic variation in the functional
66 network architecture of the human brain. We further highlight this sensitivity to estradiol
67 in a controlled replication study. Together, these findings provide insight into how brain
68 networks reorganize across the human menstrual cycle and suggest that consideration of
69 the hormonal milieu is critical for fully understanding the intrinsic dynamics of the
70 human brain.

71 **2 Materials and Methods**

72 **2.1 Participants**

73 The participant (author L.P.) is a right-handed Caucasian female, aged 23 years for
74 duration of the study. The participant had no history of neuropsychiatric diagnosis,
75 endocrine disorders, or prior head trauma. She had a history of regular menstrual cycles
76 (no missed periods, cycle occurring every 26-28 days) and had not taken hormone-based
77 medication in the 12 months prior to the first study. The participant gave written informed
78 consent and the study was approved by the University of California, Santa Barbara
79 Human Subjects Committee.

80 **2.2 Study design**

81 The participant underwent testing for 30 consecutive days, with the first test session
82 determined independently of cycle stage for maximal blindness to hormone status (Study
83 1). One year later, as part of a larger parent project, the participant repeated the 30-day

84 protocol while on a hormone regimen (0.02mg ethinyl-estradiol, 0.1mg levonorgestrel,
85 Aubra, Afaxys Pharmaceuticals), which she began 10 months prior to the start of data
86 collection (Study 2). The general procedures for both studies were identical (**Figure 1**).
87 The pharmacological regimen used in Study 2 chronically and selectively suppressed
88 progesterone while leaving estradiol dynamics largely indistinguishable from Study 1.
89 This provided a natural replication dataset in which to test the reliability of the estradiol
90 associations observed in the first study. The participant began each test session with a
91 daily questionnaire (see **Section 2.3: Behavioral assessments**), followed by an immersive
92 reality spatial navigation task (not reported here). Time-locked collection of serum and
93 whole blood started each day at 10:00am in Study 1 and 11:00am in Study 2 (± 30 min),
94 when the participant gave a blood sample. Endocrine samples were collected, at
95 minimum, after two hours of no food or drink consumption (excluding water). The
96 participant refrained from consuming caffeinated beverages before each test session. The
97 MRI session lasted one hour and consisted of structural and functional MRI sequences.

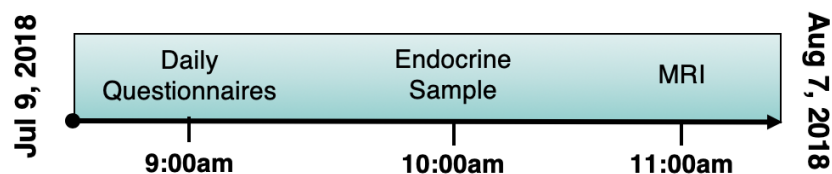


Figure 1. Timeline of data collection for the 30 experiment sessions. Endocrine and MRI assessments were collected at the same time each day to minimize time-of-day effects.

98 **2.3 Behavioral assessments**

99 To monitor state-dependent mood and lifestyle measures over the cycle, the following
100 scales (adapted to reflect the past 24 hours) were administered each morning: Perceived
101 Stress Scale (PSS) (Cohen et al., 1983), Pittsburgh Sleep Quality Index (PSQI) (Buysse et al.,
102 1989), State-Trait Anxiety Inventory for Adults (STAI) (Spielberger and Vagg, 1984), and
103 Profile of Mood States (POMS) (Pollock et al., 1979). The participant had moderate levels
104 of anxiety as determined by STAI reference ranges; however, all other measures fell within
105 the ‘normal’ standard range. Self-reported stress was marginally higher in Study 2
106 ($M_{diff} = 3.9, t(58) = 2.66, p = .046$); no other differences in mood or lifestyle measures
107 were observed between the two studies. Few significant relationships were observed
108 between hormones and state-dependent measures following FDR-correction for multiple
109 comparisons ($q < .05$)—and critically, none of these state-dependent factors were
110 associated with estradiol (**Figure 2A**). Furthermore, performance on a daily selective
111 attention task (Cohen et al., 2014) was stable across the experiment ($M = 98\%, SD = 0.01$;
112 **Figure 2B**). Taken together, there were no indications of significant shifts in behavior
113 across the cycle.

114 **2.4 Endocrine procedures**

115 A licensed phlebotomist inserted a saline-lock intravenous line into the dominant or
116 non-dominant hand or forearm daily to evaluate hypothalamic-pituitary-gonadal axis
117 hormones, including serum levels of gonadal hormones (17β -estradiol, progesterone and

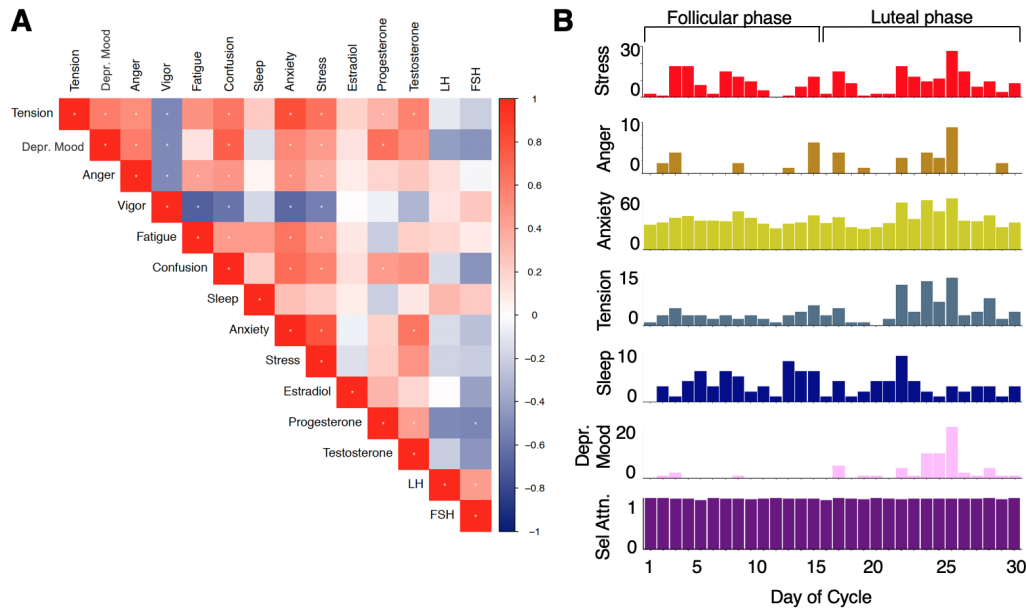


Figure 2. Behavioral variation across the 30-day experiment (Study 1). (A) Correlation plot showing relationships between mood, lifestyle measures, and sex steroid hormone concentrations. Cooler cells indicate negative correlations, warm cells indicate positive correlations, and white cells indicate no relationship. Asterisks indicate significant correlations after FDR-correction ($q < .05$). (B) Mood and lifestyle measures vary across the cycle; cognitive performance (selective attention) does not. ‘Day 1’ indicates first day of menstruation, *not* first day of experiment. Abbreviations: LH, Lutenizing hormone; FSH, Follicle-stimulating hormone.

118 testosterone) and the pituitary gonadotropins luteinizing hormone (LH) and follicle
 119 stimulating hormone (FSH). One 10cc mL blood sample was collected in a vacutainer SST
 120 (BD Diagnostic Systems) each session. The sample clotted at room temperature for 45 min
 121 until centrifugation ($2,000 \times g$ for 10 minutes) and were then aliquoted into three 1 mL
 122 microtubes. Serum samples were stored at -20°C until assayed. Serum concentrations
 123 were determined via liquid chromatography-mass spectrometry (for all steroid hormones)
 124 and immunoassay (for all gonadotropins) at the Brigham and Women’s Hospital Research
 125 Assay Core. Assay sensitivities, dynamic range, and intra-assay coefficients of variation
 126 (respectively) were as follows: estradiol, 1 pg/mL, 1–500 pg/mL, $< 5\%$ relative standard

127 deviation (*RSD*); progesterone, 0.05 ng/mL, 0.05–10 ng/mL, 9.33% *RSD*; testosterone, 1.0
128 ng/dL, 1–2000 ng/dL, < 4% *RSD*. FSH and LH levels were determined via
129 chemiluminescent assay (Beckman Coulter). The assay sensitivity, dynamic range, and the
130 intra-assay coefficient of variation were as follows: FSH, 0.2 mIU/mL, 0.2–200 mIU/mL,
131 3.1–4.3%; LH, 0.2 mIU/mL, 0.2–250 mIU/mL, 4.3–6.4%. Importantly, we note that LC-MS
132 assessments of *exogenous* hormone concentrations (attributable to the hormone regimen
133 itself) showed that serum concentrations of ethinyl estradiol were very low ($M = 0.01$
134 ng/mL; range: 0.001–0.016 ng/mL) and below 1.5 ng/mL for levonorgestrel ($M = 0.91$
135 ng/mL; range: 0.03–1.43 ng/mL): this ensures that the brain-hormone associations
136 reported below are still due to *endogenous* estradiol action in Study 2.

137 **2.5 MRI acquisition**

138 The participant underwent a daily magnetic resonance imaging scan on a Siemens 3T
139 Prisma scanner equipped with a 64-channel phased-array head coil. First, high-resolution
140 anatomical scans were acquired using a T_1 -weighted magnetization prepared rapid
141 gradient echo (MPRAGE) sequence (TR = 2500 ms, TE = 2.31 ms, TI = 934 ms, flip angle =
142 7°; 0.8 mm thickness) followed by a gradient echo fieldmap (TR = 758 ms, TE₁ = 4.92 ms,
143 TE₂ = 7.38 ms, flip angle = 60°). Next, the participant completed a 10-minute resting-state
144 fMRI scan using a T_2^* -weighted multiband echo-planar imaging (EPI) sequence sensitive
145 to the blood oxygenation level-dependent (BOLD) contrast (TR = 720 ms, TE = 37 ms, flip
146 angle = 56°, multiband factor = 8; 72 oblique slices, voxel size = 2 mm³). In an effort to
147 minimize motion, the head was secured with a custom, 3D-printed foam head case

148 (<https://caseforge.co/>) (days 8–30 of Study 1, days 1–30 of Study 2). Overall
149 motion (mean framewise displacement) was negligible (**Figure S1**), with fewer than 130
150 microns of motion on average each day. Importantly, mean framewise displacement was
151 also not correlated with estradiol concentrations (Study 1: Spearman $r = -0.06$, $p = .758$;
152 Study 2: Spearman $r = -0.33$, $p = .071$).

153 **2.6 fMRI preprocessing**

154 Initial preprocessing was performed using the Statistical Parametric Mapping 12 software
155 (SPM12, Wellcome Trust Centre for Neuroimaging, London) in Matlab. Functional data
156 were realigned and unwarped to correct for head motion and geometric deformations due
157 to motion and magnetic field inhomogeneities; the mean motion-corrected image was then
158 coregistered to the high-resolution anatomical image. All scans were then registered to a
159 subject-specific anatomical template created using Advanced Normalization Tools' (ANTs)
160 multivariate template construction (**Figure S2**). A 4 mm full-width at half-maximum
161 (FWHM) isotropic Gaussian kernel was subsequently applied to smooth the functional
162 data. Further preparation for resting-state functional connectivity was implemented using
163 in-house Matlab scripts. Global signal scaling (median = 1,000) was applied to account for
164 transient fluctuations in signal intensity across space and time, and voxelwise timeseries
165 were linearly detrended. Residual BOLD signal from each voxel was extracted after
166 removing the effects of head motion and five physiological noise components (CSF +
167 white matter signal). Motion was modeled based on the Friston-24 approach, using a
168 Volterra expansion of translational/rotational motion parameters, accounting for

169 autoregressive and nonlinear effects of head motion on the BOLD signal (Friston et al.,
170 1996). All nuisance regressors were detrended to match the BOLD timeseries. Our use of
171 coherence allows for the estimation of frequency-specific covariances in spectral
172 components below the range contaminated by physiological noise. Nevertheless, to
173 ensure the robustness of our results, we re-analyzed the data with global signal regression
174 included. This had little bearing on the overall findings. For completeness, results from
175 the GSR-based processing pipeline are provided in the **Supplementary Material**.

176 **2.7 Functional connectivity estimation**

177 Functional network nodes were defined based on a 400-region cortical
178 parcellation (Schaefer et al., 2018) and 15 regions from the Harvard-Oxford subcortical
179 atlas (<http://www.fmrib.ox.ac.uk/fsl/>). For each day, a summary timecourse
180 was extracted per node by taking the first eigenvariate across functional volumes (Friston
181 et al., 2006). These regional timeseries were then decomposed into several frequency
182 bands using a maximal overlap discrete wavelet transform (Daubechies extremal phase
183 filter, length = 8). Low-frequency fluctuations in wavelets 3–6 (~ 0.01 – 0.17 Hz) were
184 selected for subsequent connectivity analyses (Patel and Bullmore, 2016). We estimated
185 the *spectral* association between regional timeseries using magnitude-squared coherence:
186 this yielded a 415×415 functional association matrix each day, whose elements indicated
187 the strength of functional connectivity between all pairs of nodes (FDR-thresholded at
188 $q < .05$). Coherence offers several advantages over alternative methods for assessing
189 connectivity: 1) estimation of *frequency-specific covariances*, 2) *simple interpretability* (values

190 are normalized to the $[0, 1]$ interval), and 3) *robustness to temporal variability in*
191 *hemodynamics* between brain regions, which can otherwise introduce time-lag confounds
192 to connectivity estimates via Pearson correlation.

193 **2.8 Statistical analysis**

194 First, we assessed time-synchronous variation in functional connectivity associated with
195 estradiol and progesterone through a standardized regression analysis. Data were
196 Z -transformed and edgewise coherence was regressed against hormonal timeseries to
197 capture day-by-day variation in connectivity relative to hormonal fluctuations. For each
198 model, we computed robust empirical null distributions of test-statistics (β/SE) via 10,000
199 iterations of nonparametric permutation testing: under the null hypothesis of no temporal
200 association between connectivity and hormones, the coherence data at each edge were
201 randomly permuted, models were fit, and two-tailed p -values were obtained as the
202 proportion of models in which the absolute value of the permuted test statistics equaled or
203 exceeded the absolute value of the 'true' test statistics. We report edges surviving a
204 threshold of $p < .001$. We did not apply additional corrections in an effort to maximize
205 power in our small sample size; Study 2 instead offers an independent validation of the
206 observed whole-brain effects.

207 Next, we sought to capture linear dependencies between hormones and network
208 connectivity *directed in time* using vector autoregressive (VAR) models. Here we chose to
209 focus exclusively on estradiol for two reasons: 1) the highly-bimodal time-course of
210 progesterone over a natural cycle confers a considerably longer autocorrelative structure,

211 requiring many more free parameters (i.e. higher-order models, ultimately affording
212 fewer degrees of freedom); and 2) progesterone lacks an appreciable pattern of periodicity
213 in its autocovariance with network timeseries, suggesting less relevance for time-lagged
214 analysis over a single cycle. In contrast, estradiol has a much smoother time-course that is
215 well-suited for temporal evolution models such as VAR.

216 In short, VAR solves a simultaneous system of equations that fits *current* states of the
217 brain and estradiol from the *previous* states of each. For consistency, we considered only
218 *second-order* VAR models, given a fairly reliable first zero-crossing of brain/hormone
219 autocovariance functions at lag two (this was based on common criteria noted in other
220 instances of time-delayed models; Boker et al. (2014)). Fit parameters for each VAR
221 therefore reflect the following general form:

$$Brain_t = b_{1,0} + b_{1,1}Brain_{t-1} + b_{1,2}Estradiol_{t-1} + b_{1,3}Brain_{t-2} + b_{1,4}Estradiol_{t-2} + \epsilon_{1,t}$$

$$Estradiol_t = b_{2,0} + b_{2,1}Brain_{t-1} + b_{2,2}Estradiol_{t-1} + b_{2,3}Brain_{t-2} + b_{2,4}Estradiol_{t-2} + \epsilon_{2,t} \quad (1)$$

222 where error terms, $\epsilon_{i,t}$, are assumed to be uncorrelated and normally-distributed. Given
223 that the design matrix is identical for each outcome measure, they can be combined in
224 matrix form, and a least-squares solution to the system of equations can be obtained via
225 maximum likelihood.

226 With respect to brain states, we modeled both edgewise coherence and factors related
227 to macroscale network topologies. Specifically, we computed measures of *between-network*
228 integration (the participation coefficient; i.e. the average extent to which network nodes

229 are communicating with other networks over time) and *within-network* integration (global
230 efficiency, quantifying the ostensible ease of information transfer across nodes inside a
231 given network). These were derived using the relevant functions for weighted graphs in
232 the Brain Connectivity toolbox (Rubinov and Sporns, 2010). Estimation of participation
233 coefficients took the full (415×415) FDR-thresholded coherence matrices along with a
234 vector of network IDs, quantifying the extent to which each node was connected to other
235 nodes outside of its own network; summary, mean participation coefficients were then
236 obtained for each network across its constituent nodes. For global efficiencies, the $415 \times$
237 415 matrices were subdivided into smaller network-specific matrices as defined by our
238 parcellation, yielding estimates of integration only among within-network nodes.

239 Ultimately, regardless of brain measure, each VAR was estimated similarly to the
240 time-synchronous analyses described above: data were Z -scored, models were fit, and
241 model-level stats (test-statistics, R^2 , and $RMSE$) were empirically-thresholded against
242 10,000 iterations of nonparametric permutation testing. Here, however, both brain and
243 hormonal data were permuted under the null hypothesis of temporal stochasticity (i.e. no
244 autoregressive trends and no time-lagged dependencies between variables). As before, we
245 did not apply additional corrections and offer Study 2 as an independent validation set.

246 Finally, for each set of edgewise models (time-synchronous and time-lagged), we
247 attempted to disentangle both the general *direction* of hormone-related associations and
248 whether certain networks were more or less *sensitive* to hormonal fluctuations. Toward
249 that end, we took the thresholded statistical parametric maps for each model (where edges

250 are test-statistics quantifying the magnitude of association between coherence and
251 hormonal timeseries) and estimated *nodal association strengths* per graph theory's
252 treatment of signed, weighted networks. That is, positive and negative association
253 strengths were computed independently for each of the 415 nodes by summing the
254 suprathreshold positive/negative edges linked to them. We then simply assessed mean
255 association strengths (\pm 95% confidence intervals) in each direction across the various
256 networks in our parcellation.

257 Here, networks were defined by grouping the subnetworks of the 17-network
258 Schaefer parcellation, such that (for example), the A, B, and C components of the Default
259 Mode Network were treated as one network. We chose this due to the presence of a
260 unique Temporal Parietal Network in the 17-network partition, which is otherwise
261 subsumed by several other networks (Default Mode, Salience/Ventral Attention, and
262 SomatoMotor) in the 7-network partition. The subcortical nodes of the Harvard-Oxford
263 atlas were also treated as their own network, yielding a total of nine networks. These
264 definitions were thus used for computation of participation coefficients and global
265 efficiencies in network-level VAR models.

266 **2.9 Brain data visualization**

267 Statistical maps of edgewise coherence v. hormones were visualized using the Surf Ice
268 software (<https://www.nitrc.org/projects/surface/>).

269 **3 Results**

270 **3.1 Endocrine assessments**

271 Analysis of daily sex hormone (by liquid-chromatography mass-spectrometry; LC-MS)
272 and gonadotropin (by chemiluminescent immunoassay) concentrations from Study 1
273 confirmed the expected rhythmic changes of a typical menstrual cycle, with a total cycle
274 length of 27 days. Serum levels of estradiol and progesterone were lowest during menses
275 (day 1–4) and peaked in late follicular (estradiol) and late luteal (progesterone) phases
276 (**Figure 3; Table 1**). Progesterone concentrations surpassed 5 ng/mL in the luteal phase,
277 signaling an ovulatory cycle (Leiva et al., 2015). In Study 2, the participant was placed on
278 a pharmacological regimen (0.02 mg ethinyl-estradiol, 0.1 mg levonorgestrel) that
279 chronically and selectively suppressed circulating progesterone, while leaving
280 endogenous estradiol concentrations largely untouched. Estradiol dynamics in Study 2
281 ($M = 66.2$ pg/mL, range: 5–246 pg/mL) were highly similar to Study 1 ($M = 82.8$ pg/mL,
282 range: 22–264 pg/mL; $t(58) = -1.01$, $p = .32$; **Figure S3**), offering us a second dataset in
283 which to test the reliability of estradiol’s influence on intrinsic brain networks.

284 **3.2 Time-synchronous associations between sex hormones and** 285 **whole-brain functional connectivity**

286 Inspection of day-to-day similarity in whole-brain patterns of coherence (via pairwise
287 Pearson correlation) revealed moderate-to-high levels of reliability between different
288 stages of the cycle. Notably, however, one session in Study 1 (experiment day 26) was

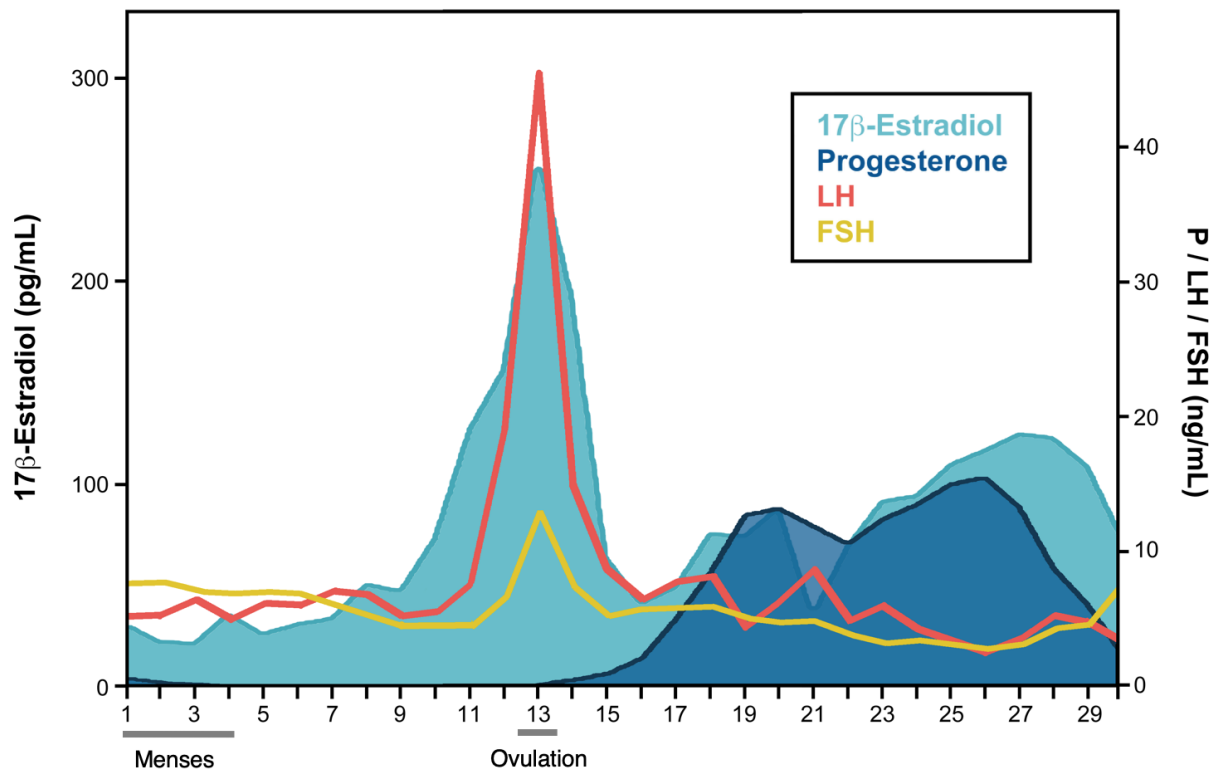


Figure 3. Participant's hormone concentrations plotted by day of cycle (Study 1). 17β -estradiol, progesterone, luteinizing hormone (LH), and follicle stimulating hormone (FSH) concentrations fell within standard ranges.

Table 1. Gonadal and pituitary hormones by cycle stage (Study 1).

	Follicular	Ovulatory	Luteal
	Mean (SD) <i>standard range</i>	Mean (SD) <i>standard range</i>	Mean (SD) <i>standard range</i>
Estradiol (pg/mL)	37.9 (15.9) 12.5–166.0	185.3 (59.0) 85.8–498.0	85.4 (26.4) 43.8–210.0
Progesterone (ng/mL)	0.2 (0.2) 0.1–0.9	0.2 (0.2) 0.1–120	9.5 (4.8) 1.8–23.9
LH (mIU/mL)	5.9 (0.7) 2.4–12.6	21.7 (16.4) 14.0–95.6	5.5 (2.0) 1.0–11.4
FSH (mIU/mL)	6.5 (1.2) 3.5–12.5	8.1 (3.6) 4.7–21.5	4.8 (1.3) 1.7–7.7

Note. Standard reference ranges based on aggregate data from Labcorp (<https://www.labcorp.com/>).

289 markedly dissimilar to the other sessions. Removal of this day from the analysis below
290 did not impact the results (**Figure S4**).

291 To further explore cycle-dependent variability, we tested the hypothesis that
292 whole-brain functional connectivity at rest is associated with intrinsic fluctuations in
293 estradiol and progesterone in a *time-synchronous* (i.e. day-by-day) fashion. Based on the
294 enriched expression of ER in frontal cortex (Wang et al., 2010), we predicted that the
295 Default Mode, Frontoparietal Control, and Dorsal Attention Networks would be most
296 sensitive to hormone fluctuations across the cycle.

297 In Study 1, we observed robust increases in coherence as a function of increasing
298 estradiol across the brain (**Figure 4A**). When summarizing the average magnitude of
299 association per network (as defined by our parcellation; **Figure 4C**), components of the
300 Temporal Parietal Network had the strongest positive associations with estradiol on

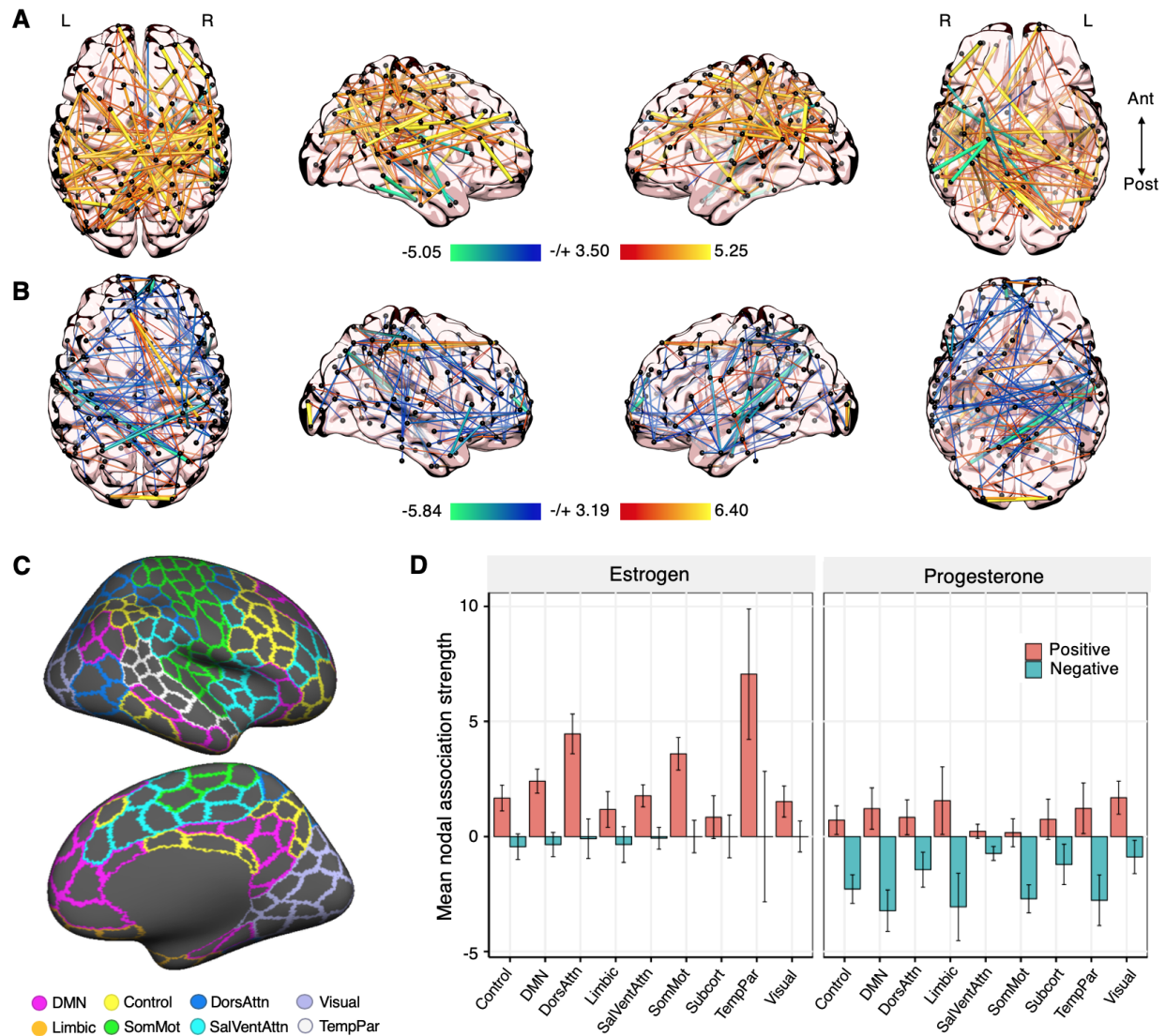


Figure 4. Whole-brain functional connectivity at rest is associated with intrinsic fluctuations in estradiol and progesterone (Study 1). (A) Time-synchronous (i.e. day-by-day) associations between estradiol and coherence. Hotter colors indicate increased coherence with higher concentrations of estradiol; cool colors indicate the reverse. Results are empirically-thresholded via 10,000 iterations of nonparametric permutation testing ($p < .001$). Nodes without significant edges are omitted for clarity. (B) Time-synchronous associations between progesterone and coherence. (C) Cortical parcellations were defined by the 400-node Schaefer atlas (shown here). An additional 15 subcortical nodes were defined from the Harvard-Oxford atlas. (D) Mean nodal association strengths by network and hormone. Error bars give 95% confidence intervals. ‘Positive’ refers to the average magnitude of positive associations (e.g. stronger coherence with higher estradiol); ‘Negative’ refers to the average magnitude of inverse associations (e.g. weaker coherence with higher estradiol). Abbreviations: DMN, Default Mode Network; DorsAttn, Dorsal Attention Network; SalVentAttn, Saliency/Ventral Attention Network; SomMot, SomatoMotor Network; TempPar, Temporal Parietal Network.

301 average, as well as the most variance (**Figure 4D**). With the exception of Subcortical nodes,
302 all networks demonstrated some level of significantly positive association on average (95%
303 CIs not intersecting zero). We observed a paucity of edges showing inverse associations
304 (connectivity decreasing while estradiol increased), with no networks demonstrating
305 significantly negative associations on average (**Figure 4D**). These findings suggest that
306 edgewise functional connectivity is primarily characterized by increased coupling as
307 estradiol rises over the course of the cycle.

308 Progesterone, by contrast, yielded a widespread pattern of inverse association across
309 the brain, such that connectivity decreased as progesterone rose (**Figure 4B**). Most
310 networks (with the exception of the Salience/Ventral Attention and SomatoMotor
311 Networks) still yielded some degree of significantly positive association over time;
312 however, the general strength of negative associations was larger in magnitude and
313 significantly nonzero across all networks (**Figure 4D**). Together, the direction of these
314 observed relationships offers a macroscale analogue to cellular-level animal models of
315 estradiol and progesterone function, consistent with proliferative (increased connectivity)
316 and reductive (decreased connectivity) effects, respectively. Re-analysis with global signal
317 regression included during preprocessing yielded a similar pattern of results (**Figure S5**),
318 suggesting that the relationships observed in Study 1 are *not* due to arbitrary changes in
319 global signal over time (e.g. due to physiological variability over the cycle).

320 Given the predominantly positive associations between connectivity and estradiol,
321 we further assessed the dependence of these effects on the estradiol surge that occurs

322 during ovulation. Removal of the ovulation window erased significant associations across
323 the brain almost entirely (**Figure S6A**), indicating that the hallmark rise of estradiol
324 during ovulation may be a key modulator of functional coupling over a reproductive
325 cycle. We then tested the reliability of these associations when estradiol fluctuations were
326 unopposed by progesterone (Study 2): this revealed similarly ubiquitous increases in
327 connectivity coincident with estradiol fluctuations (**Figure S7**). As before, removal of the
328 three highest estradiol days during the mid-cycle peak (akin to the ovulatory window
329 from Study 1) greatly reduced whole-brain associations (**Figure S6B**). Thus, whole-brain
330 functional connectivity appears highly-sensitive to estradiol regardless of reproductive
331 status.

332 **3.3 Time-lagged associations between estradiol and whole-brain** 333 **functional connectivity**

334 We then employed time-lagged methods from dynamical systems analysis to further
335 elucidate the degree to which intrinsic functional connectivity is sensitive to fluctuations
336 in estradiol: specifically, vector autoregression (VAR), which supports more *directed*
337 temporal inference than standard regression models. As described previously, we report
338 results from second-order VAR models: thus, in order to assess connectivity or hormonal
339 states on a given day of the experiment, we consider their values on both the previous day
340 (hereafter referred to as 'lag 1') and two days prior (hereafter referred to as 'lag 2').
341 Ultimately, if brain variance over time is attributable to previous states of estradiol, this

342 suggests that temporal dynamics in connectivity may be *driven* (in part) by fluctuations in
343 this hormone.

344 When assessing edgewise connectivity states, a powerful disparity emerged between
345 the brain's autoregressive effects and the effects of estradiol in Study 1. We observed vast,
346 whole-brain associations with prior hormonal states, both at lag 1 and lag 2 (**Figure 5A**).
347 Perhaps most immediately striking, the sign of these brain-hormone associations inverts
348 between lags, such that it is predominantly positive at lag 1 and predominantly negative
349 at lag 2—this holds for all networks when considering their mean nodal association
350 strengths (**Figure 5B**). We interpret this as a potential regulatory dance between brain
351 states and hormones over the course of the cycle, with estradiol perhaps playing a role in
352 maintaining both steady states (when estradiol is low) and transiently-high dynamics
353 (when estradiol rises). No such pattern emerged in the brain's autoregressive effects, with
354 sparse, low-magnitude, and predominantly negative associations at lag 1 and lag 2
355 (**Figure S8**). The observed associations between estradiol and edgewise connectivity were
356 partially unidirectional. Previous states of coherence were associated with estradiol across
357 a number of edges, intersecting all brain networks. This emerged at both lag 1 and lag 2;
358 however, unlike the lagged effects of estradiol on coherence, association strengths were
359 predominantly negative and low-magnitude (on average) at both lags (**Figure S9**).
360 Moreover—and importantly—none of the edges that informed the temporal evolution of
361 estradiol were also significantly preceded *by* estradiol at either lag (i.e. there was no
362 evidence of mutual modulation at any network edge).

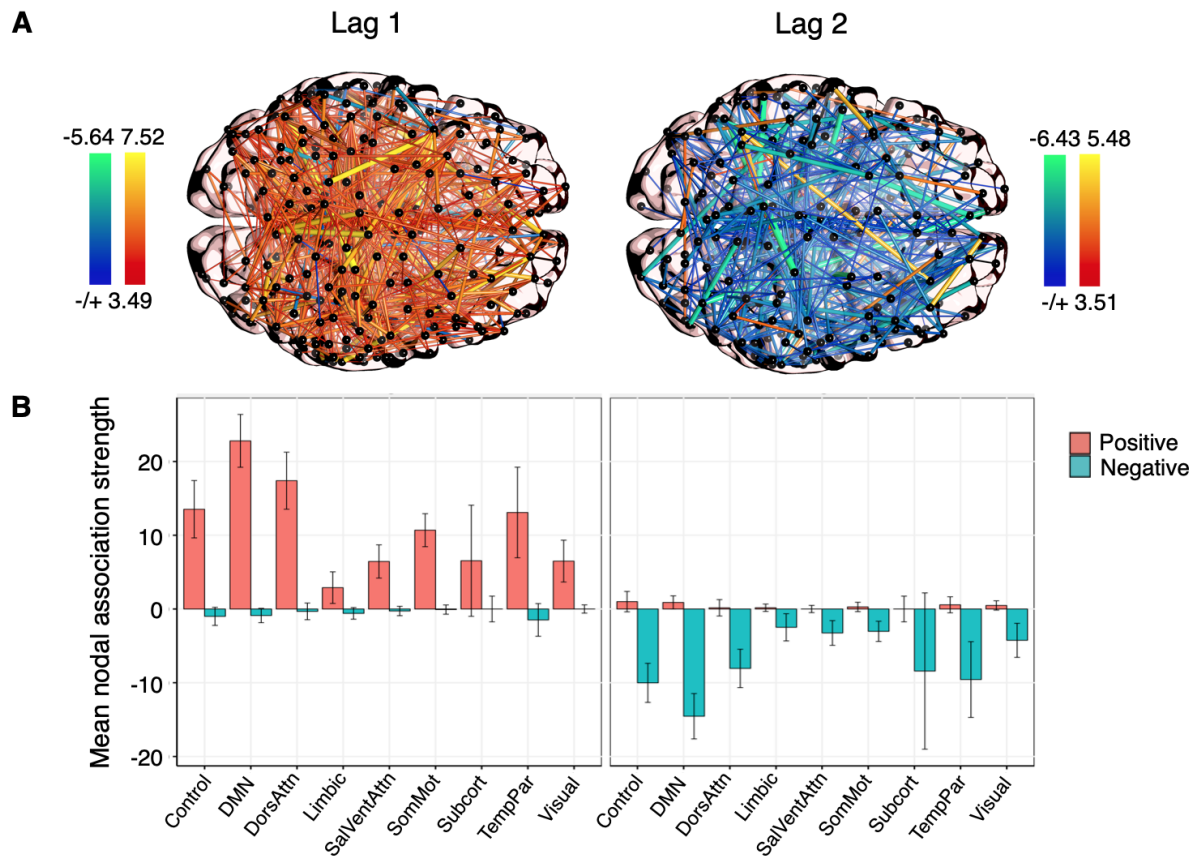


Figure 5. Whole-brain functional connectivity is linearly dependent on previous states of estradiol (Study 1). (A) Time-lagged associations between coherence and estradiol at lag 1 (*left*) and lag 2 (*right*), derived from edgewise vector autoregression models. Hotter colors indicate a predicted increase in coherence given previous concentrations of estradiol; cool colors indicate the reverse. Results are empirically-thresholded via 10,000 iterations of nonparametric permutation testing ($p < .001$). Nodes without significant edges are omitted for clarity. (B) Mean nodal association strengths by network and time lag. Error bars give 95% confidence intervals. 'Positive' refers to the average magnitude of positive associations (stronger coherence when prior states of estradiol were high); 'Negative' refers to the average magnitude of inverse associations (weaker coherence when prior states of estradiol were high).

363 We again tested the reliability of these effects in the replication sample. The
364 autoregressive trends in edgewise coherence remained sparse and low-magnitude on
365 average; however, unlike the original sample, nearly all networks demonstrated
366 significantly positive associations at lag 1, and lag 2 was dominated by negative
367 associations (**Figure S10**). Previous states of coherence also informed changes in estradiol
368 over time, but this, too, differed from the original sample at the network level. While
369 coherence at lag 1 was generally associated with decreases in estradiol across most
370 networks, several networks (including the Control, Default Mode, and Dorsal Attention
371 Networks) were associated with increases on average at lag 2 (**Figure S11**). Finally, and
372 importantly, we observed highly-robust associations between lagged states of estradiol
373 and coherence, with widespread positive associations at lag 1 and predominantly negative
374 associations at lag 2 (**Figure S12**). Curiously, in contrast to the naturally-cycling data,
375 ‘non-cognitive’ networks such as the SomatoMotor and Visual Networks demonstrated by
376 far the strongest-magnitude associations on average—particularly at lag 1. It is possible
377 that estradiol’s effects are magnified when unopposed by the inhibitory nature of
378 progesterone, a topic to be addressed in future investigations.

379 **3.4 Time-lagged associations between estradiol and functional** 380 **network topologies**

381 Given the findings above, we applied the same time-lagged framework to *topological states*
382 of brain networks in order to better capture the directionality and extent of brain-hormone
383 interactions at the mesoscopic level. These states were quantified using common graph

384 theory metrics: namely, the *participation coefficient* (an estimate of *between-network*
 385 *integration*) and *global efficiency* (an estimate of *within-network* integration). We focus on
 386 significant network-level effects below, but a full documentation of our findings is
 387 available in the **Supplementary Tables**.

Table 2. VAR model fit: Between-network participation (Study 1).

Network	Outcome	Predictor	Estimate	SE	T (p)
		Constant	0.08	0.16	0.49 (.099)
		DAN _{t-1}	0.15	0.18	0.84 (.405)
	Participation	Estradiol_{t-1}	-0.56	0.25	-2.27 (.035)
		DAN _{t-2}	-0.29	0.17	-1.71 (.093)
		Estradiol_{t-2}	0.53	0.24	2.16 (.042)
		$R^2 = 0.32$ ($p = .049$); $RMSE = 0.79$ ($p = .050$)			
Dorsal Attention		Constant	6.88×10^{-5}	0.12	0.001 (.998)
		DAN _{t-1}	0.06	0.14	0.47 (.627)
	Estradiol	Estradiol_{t-1}	1.12	0.18	6.12 (<.0001)
		DAN _{t-2}	0.03	0.13	0.24 (.806)
		Estradiol_{t-2}	-0.48	0.18	-2.65 (.007)
		$R^2 = 0.67$ ($p = .0001$); $RMSE = 0.59$ ($p = .0009$)			

Note. *p*-values empirically-derived via 10,000 iterations of nonparametric permutation testing.

388 3.4.1 Estradiol and between-network participation

389 As expected, estradiol demonstrated significant autoregressive trends across all models in
 390 Study 1. However, between-network integration was only tenuously associated with
 391 previous states of estradiol: in several intrinsic networks, overall model fit (variance
 392 accounted for, R^2 , and root mean-squared error, $RMSE$) was at best marginal compared
 393 to empirical null distributions of these statistics, and we therefore urge caution in
 394 interpreting these results. For example, in the Dorsal Attention Network (DAN; **Figure**

395 **6A-B; Table 2**), estradiol was significantly associated with between-network participation
396 both at lag 1 ($b = -0.56$, $SE = 0.25$, $t = -2.27$, $p = .035$) and at lag 2 ($b = 0.53$, $SE = 0.24$,
397 $t = 2.16$, $p = .042$). Overall fit for DAN participation, however, rested at the classical
398 frequentist threshold for significance, relative to empirical nulls ($R^2 = 0.32$, $p = .049$;
399 $RMSE = 0.79$, $p = .050$). We observed a similar pattern of results for the Default Mode
400 Network (DMN) and Limbic Network, where lagged states of estradiol were significantly
401 associated with cross-network participation, but model fit as a whole was low (see **Table**
402 **S1**).

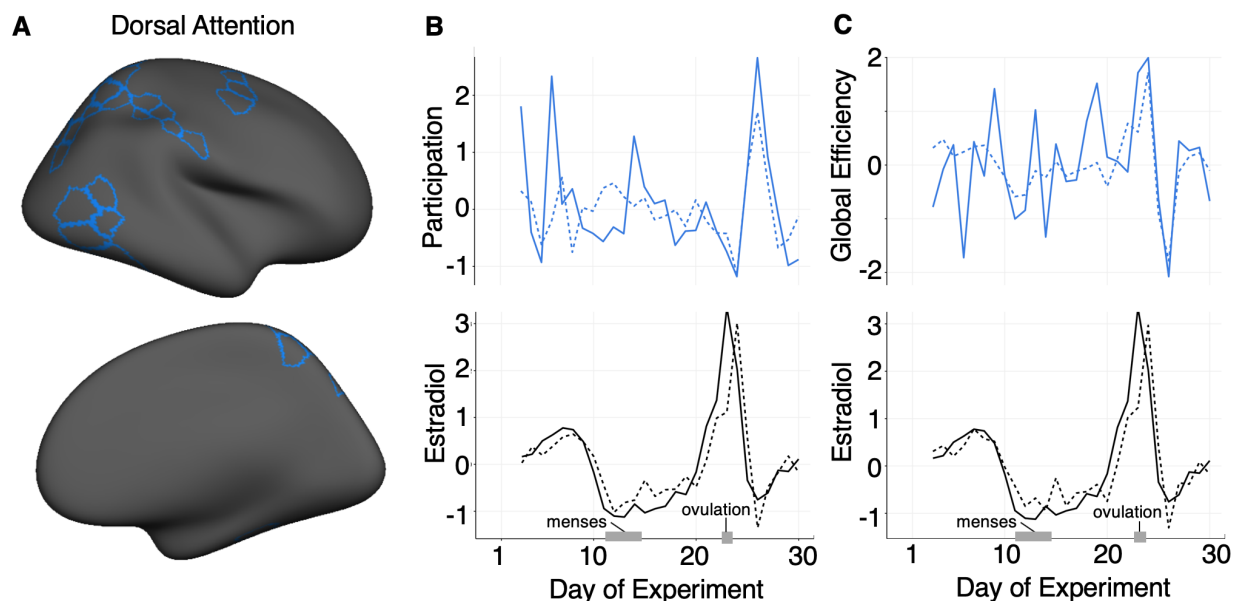


Figure 6. Dorsal Attention Network topology is driven by previous states of estradiol (Study 1). Observed data (solid lines) vs. VAR model fits (dotted lines) for between-network participation (**B, middle**) and within-network efficiency (**C, right**) in the Dorsal Attention Network (**A, left**). Timeseries for each network statistic are depicted above in (**B,C**) and estradiol for each VAR is plotted below. Data are in standardized units and begin at experiment day three, given the second-order VAR (lag of two days).

403 Importantly, we failed to replicate these effects in Study 2 under hormonal
404 suppression (**Table S2**). The autoregressive trends in estradiol were generally blunted,

405 with lag 2 now offering no predictive value. Previous states of DAN participation also
406 informed the temporal evolution of estradiol (whereas estradiol predicted DAN
407 participation in Study 1); however, this only emerged at lag 1 ($b = -0.09$, $SE = 0.04$,
408 $t = -2.08$, $p = .044$). The Limbic and Subcortical Networks additionally demonstrated
409 significant autoregressive trends at lag 1, but neither showed significant associations with
410 estradiol. In sum, the marginal model fits, along with failures to replicate in Study 2,
411 requires future investigation before robust conclusions can be drawn for between-network
412 participation.

413 3.4.2 Estradiol and global efficiency

414 In contrast to between-network integration, estradiol was more strongly associated with
415 within-network integration, both in terms of parameter estimates and overall fit. Here, the
416 Default Mode Network provided the best-fitting model in Study 1 ($R^2 = 0.50$, $p = .003$;
417 $RMSE = 0.70$, $p = .022$; **Figure 7A-B**). As before, estradiol demonstrated significant
418 autoregressive effects at lag 1 ($b = 1.15$, $SE = 0.19$, $t = 6.15$, $p < .0001$) and lag 2
419 ($b = -0.48$, $SE = 0.19$, $t = -2.50$, $p = .012$). When assessing dynamics in DMN efficiency,
420 previous states of estradiol remained significant both at lag 1 ($b = 0.98$, $SE = 0.23$,
421 $t = 3.37$, $p = .0003$) and at lag 2 ($b = -0.93$, $SE = 0.23$, $t = -4.00$, $p = .002$). Critically,
422 these effects were purely directional: prior states of Default Mode efficiency were not
423 associated with estradiol, nor did they have significant autoregressive effects, suggesting
424 that variance in topological network states (perhaps within-network integration, in
425 particular) is primarily accounted for by estradiol—not the other way around (**Table 3**).

Table 3. VAR model fit: Global efficiency (Study 1).

Network	Outcome	Predictor	Estimate	SE	$T(p)$
Default Mode	Efficiency	Constant	0.04	0.15	0.28 (.279)
		DMN _{<i>t</i>-1}	-0.04	0.16	-0.27 (.764)
		Estradiol_{<i>t</i>-1}	0.98	0.23	3.37 (.0003)
		DMN _{<i>t</i>-2}	-0.02	0.16	-0.11 (.907)
		Estradiol_{<i>t</i>-2}	-0.93	0.23	-4.00 (.002)
		$R^2 = 0.50 (p = .003); RMSE = 0.70 (p = .022)$			
Default Mode	Estradiol	Constant	0.01	0.12	0.09 (.729)
		DMN _{<i>t</i>-1}	-0.12	0.13	-0.95 (.339)
		Estradiol_{<i>t</i>-1}	1.15	0.19	6.15 (<.0001)
		DMN _{<i>t</i>-2}	-0.01	0.13	-0.08 (.930)
		Estradiol_{<i>t</i>-2}	-0.48	0.19	-2.50 (.012)
		$R^2 = 0.67 (p <.0001); RMSE = 0.58 (p = .0004)$			
Dorsal Attention	Efficiency	Constant	0.01	0.16	0.08 (.783)
		DAN _{<i>t</i>-1}	-0.11	0.18	-0.60 (.562)
		Estradiol_{<i>t</i>-1}	0.84	0.25	3.35 (.002)
		DAN _{<i>t</i>-2}	-0.10	0.18	-0.58 (.571)
		Estradiol_{<i>t</i>-2}	-0.67	0.16	-2.57 (.017)
		$R^2 = 0.37 (p = .002); RMSE = 0.77 (p = .023)$			
Dorsal Attention	Estradiol	Constant	0.01	0.12	0.06 (.808)
		DAN _{<i>t</i>-1}	-0.17	0.13	-1.29 (.207)
		Estradiol_{<i>t</i>-1}	1.17	0.19	6.30 (<.0001)
		DAN _{<i>t</i>-2}	-0.02	0.13	0.24 (.806)
		Estradiol_{<i>t</i>-2}	-0.48	0.18	-2.49 (.011)
		$R^2 = 0.68 (p <.0001); RMSE = 0.57 (p = .0004)$			

Note. *p*-values empirically-derived via 10,000 iterations of nonparametric permutation testing.

426 We observed a similar pattern of results in the Dorsal Attention Network ($R^2 = 0.37$,
427 $p = .022$; $RMSE = 0.77$, $p = .023$; **Figure 6C**; **Table 3**). Estradiol again demonstrated
428 significant autoregressive trends at lag 1 ($b = 1.17$, $SE = 0.19$, $t = 6.30$, $p < .0001$) and lag
429 2 ($b = -0.48$, $SE = 0.19$, $t = -2.49$, $p = .011$), as well as significant lagged associations
430 with DAN efficiency both at lag 1 ($b = 0.84$, $SE = 0.25$, $t = 3.35$, $p = .002$) and at lag 2

431 ($b = -0.67, SE = 0.16, t = -2.57, p = .017$). As above, Dorsal Attention efficiency had no
432 significant effects on estradiol, nor were there significant autoregressive effects of the
433 network on itself.

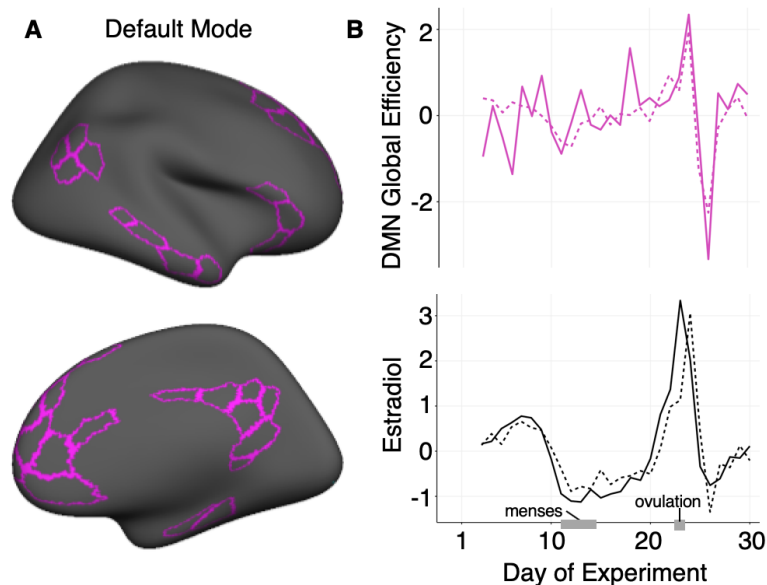


Figure 7. Default Mode Network topology is driven by previous states of estradiol (Study 1). Observed data (solid lines) vs. VAR model fits (dotted lines) for within-network efficiency (**B, right**) in the Default Mode Network (**A, left**). The efficiency timeseries is depicted above in (**B**) and estradiol is plotted below. Data are in standardized units and begin at experiment day three, given the second-order VAR (lag of two days).

434 The Control and Temporal Parietal networks also yielded partial support for
435 time-dependent modulation of efficiency by estradiol (Control $R^2 = 0.34, p = .039$;
436 Temporal Parietal $R^2 = 0.36, p = .026$). The time-lagged effects of estradiol followed the

437 trends observed above; however, the overall model fit (with respect to prediction error)
438 was not significantly better than their empirical nulls (Control $RMSE = 0.83$, $p = .133$;
439 Temporal Parietal $RMSE = 0.79$, $p = .057$). Estradiol did not explain a significant
440 proportion of variance in efficiency for any other networks in Study 1 (**Table S3**).

441 In contrast to between-network participation, within-network efficiency yielded
442 stronger evidence for replication in Study 2. The DMN again demonstrated the strongest
443 model fit ($R^2 = 0.38$, $p = .019$; $RMSE = 0.74$, $p = .011$), with estradiol informing
444 fluctuations in DMN efficiency both at lag 1 ($b = 2.48$, $SE = 0.75$, $t = 3.29$, $p = .003$) and
445 lag 2 ($b = -2.69$, $SE = 0.91$, $t = -2.94$, $p = .009$). We also observed a significant
446 autoregressive effect of DMN efficiency at lag 2 ($b = -0.45$, $SE = 0.19$, $t = -2.41$,
447 $p = .027$), but not at lag 1. In the DAN, significant model fit was achieved with respect to
448 prediction error ($RMSE = 0.79$, $p = .045$), but variance accounted for was marginal
449 relative to empirical nulls ($R^2 = 0.32$, $p = .052$). Accordingly, estradiol significantly
450 associated with DAN efficiency at lag 1 ($b = 1.88$, $SE = 0.79$, $t = 2.37$, $p = .026$) but not at
451 lag 2. Finally, previous states of estradiol (both lags 1 and 2) significantly informed
452 efficiency in the Control, Salience / Ventral Attention, SomatoMotor, and Subcortical
453 Networks; however, aside from the SomatoMotor Network ($R^2 = 0.34$, $p = .039$;
454 $RMSE = 0.76$, $p = .018$), overall fit in these models was nonsignificant (**Table S4**). Thus,
455 while we observed trends largely consistent with Study 1 (with respect to DMN and DAN
456 efficiency), there may be additional network-level effects in a neuroendocrine system
457 unopposed by progesterone, warranting future investigation.

458 **4 Discussion**

459 In this dense-sampling, deep-phenotyping project, a naturally-cycling female underwent
460 resting state fMRI and venipuncture for 30 consecutive days, capturing the dynamic
461 endocrine changes that unfold over the course of a complete menstrual cycle.

462 Time-synchronous analyses illustrate estradiol's widespread associations with cortical
463 network dynamics, spanning all but one of the networks in our parcellation. Time-lagged
464 vector autoregressive models tested the temporal directionality of these effects, suggesting
465 that intrinsic network dynamics may be partially driven by recent states of estradiol,
466 particularly with respect to within-network connectivity: global efficiency in the Default
467 Mode and Dorsal Attention Networks exhibited the strongest associations with
468 fluctuations in estradiol, replicated between Studies 1 and 2. In contrast to estradiol's
469 proliferative effects, progesterone was primarily associated with reduced coherence across
470 the whole brain. Findings from a replication dataset further establish estradiol's impact on
471 large-scale cortical dynamics. Critically, removal of high estradiol days in both studies
472 reduced associations across the brain, suggesting that the hallmark rise of estradiol
473 surrounding the ovulatory window may be a key modulator of functional coupling
474 during the reproductive cycle (**Figure S6**). These results reveal the rhythmic nature in
475 which brain networks reorganize across the human menstrual cycle.

476 The network neuroscience community has begun to probe functional networks over
477 the timescale of weeks, months, and years to understand the extent to which brain
478 networks vary between individuals or within an individual over time (Betzel et al., 2019;

479 Finn et al., 2015; Gordon et al., 2017; Horien et al., 2019; Poldrack et al., 2015; Seitzman
480 et al., 2019). These studies indicate that functional networks are dominated by common
481 organizational principles and stable individual features, especially in frontoparietal
482 control regions (Finn et al., 2015; Gordon et al., 2017; Gratton et al., 2018a; Horien et al.,
483 2019). An overlooked feature of these regions is that they are populated with estrogen and
484 progesterone receptors and are exquisitely sensitivity to major changes in sex hormone
485 concentrations (Berman et al., 1997; Hampson and Morley, 2013; Jacobs and D'Esposito,
486 2011; Jacobs et al., 2016a,b; Shanmugan and Epperson, 2014). Our findings demonstrate
487 significant effects of estradiol on functional network nodes belonging to the DMN, DAN,
488 and FCN that overlap with ER-rich regions of the brain, including medial/dorsal
489 PFC (Wang et al., 2010; Yeo et al., 2011). This study merges the network neuroscience and
490 endocrinology disciplines by demonstrating that higher-order processing systems are
491 modulated by day-to-day changes in sex hormones over the timescale of one month.

492 **4.1 Sex hormones regulate brain organization across species**

493 Animal studies offer unambiguous evidence that sex steroid hormones shape the synaptic
494 organization of the brain, particularly in regions that support higher order cognitive
495 functions (Frick et al., 2018, 2015; Galea et al., 2017; Hara et al., 2015; Woolley and
496 McEwen, 1993). In rodents, estradiol increases fast-spiking interneuron excitability in
497 deep cortical layers (Clemens et al., 2019). In nonhuman primates, whose reproductive
498 cycle length is similar to humans, estradiol increases the number of synapses in PFC (Hara
499 et al., 2015). Recently, this body of work has also begun to uncover the functional

500 significance of sinusoidal *changes* in estradiol. For example, estradiol's ability to promote
501 PFC spinogenesis in ovariectomized animals occurs *only if* the hormone add-back regime
502 mirrors the cyclic pattern of estradiol release typical of the macaque menstrual cycle (Hao
503 et al., 2006; Ohm et al., 2012). Pairing estradiol with cyclic administration of progesterone
504 blunts this increase in spine density (Ohm et al., 2012). In the hippocampus, progesterone
505 has a similar inhibitory effect on dendritic spines, blocking the proliferative effects of
506 estradiol 6 hours after administration (Woolley and McEwen, 1993). Together, the
507 preclinical literature suggests that progesterone antagonizes the largely proliferative
508 effects of estradiol (for review, see Brinton et al. (2008)). We observed a similar
509 relationship, albeit at a different spatiotemporal resolution, with estradiol demonstrating
510 positive associations with coherence across numerous cortical networks and progesterone
511 having an opposite, negative association on average. In sum, animal studies have
512 identified estradiol's influence on regional brain organization at the microscopic scale.
513 Here, we show that estradiol and progesterone may have analogous effects evident at the
514 mesoscopic scale of whole-brain connectivity, measured by spectral coherence, and
515 macroscopic features of network topology.

516 **4.2 Resting-state network characteristics differ by cycle stage**

517 Group-based and sparser-sampling neuroimaging studies provide further support that
518 cycle stage and sex hormones impact resting state networks (De Bondt et al., 2015;
519 Lisofsky et al., 2015; Petersen et al., 2014; Syan et al., 2017; Weis et al., 2019). For instance,
520 Petersen et al. (2014) demonstrated that women sampled in the follicular stage had greater

521 connectivity within default mode and executive control networks compared to those
522 sampled in the luteal stage. Lisofsky et al. (2015) studied women four times across their
523 menstrual cycles, observing significant increases in connectivity between the
524 hippocampus and superior parietal lobule during the late follicular phase. However,
525 recent work by Weis et al. (2019) provides compelling yet contrasting evidence for sex
526 hormones' relationships with resting-state functional connectivity: studying women three
527 times across the cycle, their group observed heightened connectivity between a region of
528 the left frontal cortex and the DMN during menstruation when estradiol levels are lowest.
529 Inconsistencies between studies could be due to a number of factors such as differences in
530 cycle staging methods, divergent functional connectivity estimation methods, or
531 unaccounted for intra/inter-individual variability (Beltz and Moser, 2019). Our results
532 suggest that failure to properly capture the complete ovulatory window, when estradiol
533 levels rapidly rise, could lead to skewed estimates of stability within functional brain
534 networks across the menstrual cycle (Hjelmervik et al., 2014). As such, dense-sampling
535 studies provide a novel solution to capturing pivotal moments experienced across a
536 complete human menstrual cycle. Arélin et al. (2015) sampled an individual every 2-3
537 days across four cycles and found that progesterone was associated with increased
538 connectivity between the hippocampus, dorsolateral PFC and sensorimotor cortex,
539 providing compelling evidence that inter-regional connectivity varies over the cycle. This
540 particular dense-sampling approach allowed the authors to examine brain-hormone
541 relationships while accounting for intra-individual cycle variation.

542 Estradiol is capable of inducing rapid, non-genomic effects and slower,
543 genomic-effects on the central nervous system. For example, spine density on
544 hippocampal neurons varies by ~30% over the rodent estrous cycle. In-vivo MRI evidence
545 in mice demonstrates that these hormone-mediated changes can occur rapidly, with
546 differences detectable within a 24-hour period. To capture time-synchronous (rapid) and
547 time-lagged (delayed) effects of sex steroid hormones, we expanded upon the approach of
548 Arélin et al. (2015) by sampling an individual every 24 hours for 30 consecutive days. Our
549 results illuminate how time-synchronous correlations and time-lagged computational
550 approaches reveal unique aspects of where and how hormones exert their effect on the
551 brain's intrinsic networks. Time-synchronous analyses illustrated contemporaneous,
552 zero-lag associations between estradiol, progesterone, and whole-brain connectivity. The
553 introduction of lagged states in VAR allowed us to examine the temporal directionality of
554 those relationships, suggest that recent fluctuations in estradiol (within two days) inform
555 current brain states—this raises the interesting possibility that estradiol may play a partial
556 role in driving changes in connectivity, particularly in the DMN and DAN.

557 **4.3 Neurobiological interpretations of hormonal effects and future** 558 **studies**

559 The following considerations could enhance the interpretation of these data. First, our
560 investigation deeply sampled a single woman, limiting our ability to generalize these
561 findings to other individuals. To enrich our understanding of the relationship between sex
562 hormones and brain function, this dense-sampling approach should be extended to a

563 diverse sample of women. Doing so will allow us to examine the consistency of our results
564 with respect to inter-individual differences in network organization over the menstrual
565 cycle. Additionally, examining network organization during a state of complete hormone
566 suppression would afford a valuable comparison, as certain oral hormonal contraceptives
567 suppress the production of *both* ovarian hormones. If dynamic changes in estradiol are
568 *facilitating* increases in resting connectivity, we expect hormonally-suppressed individuals
569 to show less dynamic modulation of functional brain networks over time. Given the
570 widespread use of oral hormonal contraceptives (100 million users worldwide), it is
571 critical to determine whether sweeping changes to an individual's endocrine state impacts
572 brain states and whether this, in turn, has any bearing on cognition.

573 Second, in freely-cycling individuals, sex hormones function as
574 proportionally-coupled *nonlinear* oscillators (Boker et al., 2014). Within-person cycle
575 variability is almost as large as between-person cycle variability, which hints that there are
576 highly-complex hormonal interactions within this regulatory system (Boker et al., 2014;
577 Fehring et al., 2006). The VAR models we have explored reveal *linear* dependencies
578 between brain states and hormones, but other dynamical systems methods (e.g. coupled
579 latent differential equations) may offer more biophysical validity (Boker et al., 2014).
580 However, the current sample size precludes robust estimation of such a model.

581 Third, while permutation tests have been used as empirical null models for
582 VAR (Hyvärinen et al., 2010) and its statistical relatives (e.g. Granger causality; Barnett
583 and Seth (2014)), the practice of temporally-scrambling a timeseries will drastically alter

584 its autocorrelative structure and potentially skew observed dependencies over time.
585 Phase-shifting, surrogate data tests such as the amplitude adjusted Fourier transform
586 (AAFT) may offer more robust null distributions. However, AAFT also makes strong
587 distributional assumptions about the original timeseries (Gaussian normality) that,
588 unfortunately, are not met by these data. Additionally, the small sample size over a single
589 cycle precludes the ability to derive robust surrogate realizations of the timeseries. While
590 AAFT is arguably an *ideal* procedure for analyses such as those reported here, these data
591 simply cannot meet the assumptions required for valid surrogate testing and thus is a
592 major limitation within the current study. Future investigations involving larger samples
593 of women over several cycles that allow implementation of such models will be critical.

594 Fourth, while coherence is theoretically robust to timing differences in the
595 hemodynamic response function, hormones can affect the vascular system (Krause et al.,
596 2006). Therefore, changes in coherence may be due to vascular artifacts that affect the
597 hemodynamic response in fMRI, rather than being *neurally*-relevant. Future investigations
598 exploring the assumptions of hemodynamics in relation to sex steroid hormone
599 concentrations will add clarity as to how the vascular system's response to hormones
600 might influence large-scale brain function.

601 Fifth, these findings contribute to an emerging body of work on estradiol's ability to
602 enhance the efficiency of PFC-based cortical circuits. In cycling women performing a
603 working memory task, PFC activity is exaggerated under low estradiol conditions and
604 reduced under high estradiol conditions (Jacobs and D'Esposito, 2011). The same pattern

605 is observed decades later in life: as estradiol production decreases over the menopausal
606 transition, working memory-related PFC activity becomes more exaggerated, despite no
607 difference in working memory performance (Jacobs et al., 2016a). Here, we show that
608 day-to-day changes in estradiol enhance the global efficiency of functional networks, with
609 pronounced effects in networks (DMN and FCN) that encompass major regions of the
610 PFC (Schaefer et al., 2018; Yeo et al., 2011). Together, these findings suggest that estradiol
611 generates a neurally efficient PFC response at rest and while engaging in a cognitive task.
612 Estradiol's action may occur by enhancing dopamine synthesis and release (Creutz and
613 Kritzer, 2002). The PFC is innervated by midbrain dopaminergic neurons that form the
614 mesocortical dopamine track (Kritzer and Creutz, 2008). Decades of evidence have
615 established that dopamine signaling enhances the signal-to-noise ratio of PFC pyramidal
616 neurons (Williams and Goldman-Rakic, 1995) and drives cortical efficiency (Cai and
617 Arnsten, 1997; Gibbs and D'Esposito, 2005; Granon et al., 2000; Vijayraghavan et al., 2007).
618 In turn, estradiol enhances dopamine release and modifies the basal firing rate of
619 dopaminergic neurons (Becker, 1990; Pasqualini et al., 1995; Thompson and Moss, 1994), a
620 possible neurobiological mechanism by which alterations in estradiol could impact
621 cortical efficiency. Future multimodal neuroimaging studies in humans can clarify the link
622 between estradiol's ability to stimulate dopamine release and the hormone's ability to
623 drive cortical efficiency within PFC circuits.

624 Sixth, we observed surprisingly few autoregressive effects in brain measures across
625 our time-lagged models. This was despite relatively strong day-to-day similarity in

626 whole-brain patterns of connectivity (**Figure S3**), and clear evidence for autocorrelation
627 when assessing the brain data in an independent, univariate fashion. Thus, the
628 incorporation of sex hormones into a time-lagged modeling framework attributed more
629 temporal variability in the brain to fluctuations in hormone concentrations. Nevertheless,
630 an ongoing debate within the network neuroscience community surrounds test-retest
631 reliability in resting-state functional connectivity analyses. Some studies state that large
632 amounts of data (> 20 minutes) are necessary for test-retest reliability (Gratton et al.,
633 2018a; Noble et al., 2017), while others argue that reliability can be derived from shorter
634 (5-15 minutes) scans (Birn et al., 2013; Van Dijk et al., 2010). We are limited in our ability to
635 assess whether the ostensibly-weak autoregressive trends suggested by our time-lagged
636 models would be replicated under longer scanning durations and hope future work
637 addresses this issue.

638 Finally, we chose to apply a well-established group-based atlas (Schaefer et al., 2018)
639 to improve generalizability to other individuals, as a key goal of our investigation was to
640 demonstrate how sex steroid hormones explain variability in intrinsic network topologies
641 based on regional definitions shown to be reliable across thousands of individuals
642 (Schaefer et al., 2018; Yeo et al., 2011). Yet, group-based atlases can lead to potential loss in
643 individual-level specificity, and recent work has demonstrated that fixed atlases may not
644 capture underlying reconfigurations in the parcellations themselves within an
645 individual (Bijsterbosch et al., 2019; Salehi et al., 2020a,b). Therefore, future work using
646 individual-derived functional networks will be necessary to determine whether spatial

647 reconfigurations in *parcellations* emerge as a function of the menstrual cycle, over and
648 above the influence of state or trait features. Relatedly, variation in analytic pipelines of
649 brain imaging data can lead to divergent conclusions even within the same
650 dataset (Botvinik-Nezer et al., 2020); for complete transparency, we are committed to
651 making all neuroimaging data and code publicly available so that other investigators can
652 assess these brain-hormone associations using their preferred methods (see **Data**
653 **availability**).

654 **4.4 Estradiol modulates global efficiency in estrogen-receptor rich** 655 **brain regions**

656 Using dense-sampling approaches to probe brain-hormone interactions could reveal
657 organizational principles of the functional connectome previously unknown, transforming
658 our understanding of how hormones influence brain states. Human studies implicate sex
659 steroids in the regulation of brain structure and function, particularly within ER-rich
660 regions like the PFC and hippocampus (Berman et al., 1997; Girard et al., 2017; Hampson
661 and Morley, 2013; Jacobs and D'Esposito, 2011; Jacobs et al., 2015, 2016a,b; Shanmugan
662 and Epperson, 2014; Zeydan et al., 2019), and yet, the neuroendocrine basis of the brain's
663 network organization remains understudied. Here, we used a network neuroscience
664 approach to investigate how hormones modulate the topological integration of functional
665 networks across the brain, showing that estradiol is associated with increased coherence
666 across broad swaths of cortex that extend beyond regions with established ER expression.
667 At the network level, estradiol enhances within-network efficiency (with robust effects in

668 DAN and DMN) and, to a lesser extent, modulates between-network participation
669 (although critically, this finding failed to replicate in Study 2). Moving forward, a complete
670 mapping of ER/PR expression in the human brain will be essential for our understanding
671 and interpretation of brain-hormone interactions. Furthermore, this dense-sampling
672 approach could be applied to brain imaging studies of other major neuroendocrine
673 transitions, such as pubertal development and reproductive aging (e.g. menopause).

674 **4.5 Implications of hormonally regulated network dynamics for** 675 **cognition**

676 An overarching goal of network neuroscience is to understand how coordinated activity
677 within and between functional brain networks supports cognition. Increased global
678 efficiency is thought to optimize a cognitive workspace (Bullmore and Bassett, 2011),
679 while between-network connectivity may be integral for integrating top-down signals
680 from multiple higher-order control hubs (Gratton et al., 2018b). The dynamic
681 reconfiguration of functional brain networks is implicated in performance across cognitive
682 domains, including motor learning (Bassett et al., 2011; Mattar et al., 2018), cognitive
683 control (Seeley et al., 2007), and memory (Fornito et al., 2012). Our results suggest that the
684 within-network connectivity of these large-scale networks is temporally-dependent on
685 hormone fluctuations across the human menstrual cycle, particularly in states of high
686 estradiol (e.g. ovulation). Future studies should consider whether these network changes
687 confer advantages to domain-general or domain-specific cognitive performance.
688 Accordingly, future planned analyses from this dataset will incorporate task-based fMRI

689 to determine whether the brain's network architecture is similarly-variable across the
690 cycle when engaging in a cognitive task, or in the dynamic reconfiguration that occurs
691 when transitioning from rest to task.

692 **4.6 Implications of hormonally regulated network dynamics for** 693 **clinical diagnoses**

694 Clinical network neuroscience seeks to understand how large-scale brain networks differ
695 between healthy and patient populations (Fox and Greicius, 2010; Hallquist and Hillary,
696 2019). Disruptions in functional brain networks are implicated in a number of
697 neurodegenerative and neuropsychiatric disorders: intrinsic connectivity abnormalities in
698 the DMN are evident in major depressive disorder (Greicius et al., 2007) and Alzheimer's
699 disease (Buckner et al., 2009). Notably, these conditions have a sex-skewed disease
700 prevalence: women are at twice the risk for depression and make up two-thirds of the
701 Alzheimer's disease patient population (Nebel et al., 2018). Here, we show that estradiol
702 modulates efficiency within the DMN and DAN, with pronounced rises in estradiol
703 significantly preceding increases in within-network coherence. A long history of clinical
704 evidence further implicates sex hormones in the development of mood disorders (Plotsky
705 et al., 1998; Rubinow and Schmidt, 2006; Young and Korszun, 2002). For example, the
706 incidence of major depression increases with pubertal onset in females (Angold and
707 Costello, 2006), chronic use of hormonal contraceptives (Young et al., 2007), the
708 postpartum period (Bloch et al., 2000), and perimenopause (Schmidt and Rubinow, 2009).
709 Moving forward, a network neuroscience approach might have greater success at

710 identifying the large-scale network disturbances that underlie, or predict, the emergence
711 of disease symptomology by incorporating sex-dependent variables (such as endocrine
712 status) into clinical models. This may be particularly true during periods of profound
713 neuroendocrine change (e.g. puberty, pregnancy, menopause, and use of hormone-based
714 medications, reviewed by Taylor et al. (2019)) given that these hormonal transitions are
715 associated with a heightened risk for mood disorders.

716 **5 Conclusion**

717 In sum, endogenous hormone fluctuations over the reproductive cycle have a robust
718 impact on the intrinsic network properties of the human brain. Despite over 20 years of
719 evidence from rodent, nonhuman primate, and human studies demonstrating the
720 tightly-coupled relationship between our endocrine and nervous systems (Beltz and
721 Moser, 2019; Hara et al., 2015; McEwen, 2018), the field of network neuroscience has
722 largely overlooked how endocrine factors shape the brain. The dynamic endocrine
723 changes that unfold over the menstrual cycle are a natural feature of half of the world's
724 population. Understanding how these changes in sex hormones might influence the
725 large-scale functional architecture of the human brain is imperative for our basic
726 understanding of the brain and for women's health.

727 **End Notes**

728 **Acknowledgements.** This work was supported by the Brain and Behavior Research
729 Foundation (EGJ), the California Nanosystems Institute (EGJ), the Institute for
730 Collaborative Biotechnologies through grant W911NF-19-D-0001 from the U.S. Army
731 Research Office (MBM), and the Rutherford B. Fett Fund (STG). Thanks to Mario Mendoza
732 for phlebotomy and MRI assistance. We would also like to thank Courtney Kenyon,
733 Maggie Hayes, and Morgan Fitzgerald for assistance with data collection.

734 **Author contributions.** The overall study was conceived by L.P., C.M.T., S.T.G., and
735 E.G.J.; L.P., T.S., E.L., C.M.T., S.Y., and E.G.J. performed the experiments; data analysis
736 strategy was conceived by T.S. and L.P. and implemented by T.S.; L.P., T.S., and E.G.J.
737 wrote the manuscript; E.L., C.M.T., S.Y., M.B.M., and S.T.G. edited the manuscript.

738 **Data/code availability.** The full dataset consists of daily mood, diet, and behavioral
739 assessments, task-based and resting-state fMRI, structural MRI, and serum assessments of
740 pituitary gonadotropins and ovarian sex hormones. The dataset and all analysis code will
741 be made publicly available upon publication.

742 **Conflict of interest.** The authors declare no competing financial interests.

References

- Angold A**, Costello EJ. Puberty and depression. *Child Adolesc Psychiatr Clin N Am*. 2006; 15(4):919–937. doi: 10.1016/j.chc.2006.05.013.
- Arélin K**, Mueller K, Barth C, Rekkas PV, Kratzsch J, Burmann I, Villringer A, Sacher J. Progesterone mediates brain functional connectivity changes during the menstrual cycle—a pilot resting state MRI study. *Front Neurosci*. 2015; 9:44. doi: 10.3389/fnins.2015.00044.
- Barnett L**, Seth AK. The MVGC multivariate Granger causality toolbox: A new approach to Granger-causal inference. *Journal of Neuroscience Methods*. 2014; 223:50 – 68.
- Bassett DS**, Wymbs NF, Porter MA, Mucha PJ, Carlson JM, Grafton ST. Dynamic reconfiguration of human brain networks during learning. *Proc Natl Acad Sci USA*. 2011; 108(18):7641–7646. doi: 10.1073/pnas.1018985108.
- Becker JB**. Estrogen rapidly potentiates amphetamine-induced striatal dopamine release and rotational behavior during microdialysis. *Neurosci Lett*. 1990; 118(2):169–171. doi: 10.1016/0304-3940(90)90618-j.
- Beltz AM**, Moser JS. Ovarian hormones: A long overlooked but critical contributor to cognitive brain structures and function. *Ann N Y Acad Sci*. 2019; doi: 10.1111/nyas.14255.
- Berman KF**, Schmidt PJ, Rubinow DR, Danaceau MA, Van Horn JD, Esposito G, Ostrem JL, Weinberger DR. Modulation of cognition-specific cortical activity by gonadal steroids: a positron-emission tomography study in women. *Proc Natl Acad Sci USA*. 1997; 94(16):8836–8841. doi: 10.1073/pnas.94.16.8836.
- Betzel RF**, Bertolero MA, Gordon EM, Gratton C, Dosenbach NUF, Bassett DS. The community structure of functional brain networks exhibits scale-specific patterns of inter- and intra-subject variability. *Neuroimage*. 2019; doi: 10.1016/j.neuroimage.2019.07.003.

Bijsterbosch JD, Beckmann CF, Woolrich MW, Smith SM, Harrison SJ. The relationship between spatial configuration and functional connectivity of brain regions revisited. *Elife*. 2019; 8.

Birn RM, Molloy EK, Patriat R, Parker T, Meier TB, Kirk GR, Nair VA, Meyerand ME, Prabhakaran V. The effect of scan length on the reliability of resting-state fMRI connectivity estimates. *Neuroimage*. 2013 12; 83:550–558.

Bloch M, Schmidt PJ, Danaceau M, Murphy J, Nieman L, Rubinow DR. Effects of gonadal steroids in women with a history of postpartum depression. *Am J Psychiatry*. 2000; 157(6):924–930. doi: 10.1176/appi.ajp.157.6.924.

Boker SM, Neale MC, Klump KL. In: Molenaar PC, Lerner R, Newll K, editors. A differential equations model for the ovarian hormone cycle. New York: Guilford Press; 2014. p. 369–391.

Botvinik-Nezer R, Holzmeister F, Camerer CF, Dreber A, Huber J, Johannesson M, Kirchler M, Iwanir R, Mumford JA, Adcock RA, Avesani P, Baczkowski BM, Bajracharya A, Bakst L, Ball S, Barilari M, Bault N, Beaton D, Beitner J, Benoit RG, et al. Variability in the analysis of a single neuroimaging dataset by many teams. *Nature*. 2020; .

Brinton RD, Thompson RF, Foy MR, Baudry M, Wang J, Finch CE, Morgan TE, Pike CJ, Mack WJ, Stanczyk FZ, Nilsen J. Progesterone receptors: form and function in brain. *Front Neuroendocrinol*. 2008; 29(2):313–339. doi: 10.1016/j.yfrne.2008.02.001.

Buckner RL, Sepulcre J, Talukdar T, Krienen FM, Liu H, Hedden T, Andrews-Hanna JR, Sperling RA, Johnson KA. Cortical hubs revealed by intrinsic functional connectivity: mapping, assessment of stability, and relation to Alzheimer’s disease. *J Neurosci*. 2009; 29(6):1860–1873. doi: 10.1523/JNEUROSCI.5062-08.2009.

Bullmore ET, Bassett DS. Brain graphs: graphical models of the human brain connectome. *Annu Rev Clin Psychol*. 2011; 7:113–140. doi: 10.1146/annurev-clinpsy-040510-143934.

- Buysse DJ**, Reynolds CF, Monk TH, Berman SR, Kupfer DJ. The Pittsburgh Sleep Quality Index: a new instrument for psychiatric practice and research. *Psychiatry Res.* 1989; 28(2):193–213. doi: 10.1016/0165-1781(89)90047-4.
- Cai JX**, Arnsten AF. Dose-dependent effects of the dopamine D1 receptor agonists A77636 or SKF81297 on spatial working memory in aged monkeys. *J Pharmacol Exp Ther.* 1997; 283(1):183–189.
- Clemens AM**, Lenschow C, Beed P, Li L, Sammons R, Naumann RK, Wang H, Schmitz D, Brecht M. Estrus-cycle regulation of cortical inhibition. *Curr Biol.* 2019; 29(4):605–615. doi: 10.1016/j.cub.2019.01.045.
- Cohen JR**, Gallen CL, Jacobs EG, Lee TG, D’Esposito M. Quantifying the reconfiguration of intrinsic networks during working memory. *PLOS ONE.* 2014; 9(9):1–8. doi: 10.1371/journal.pone.0106636.
- Cohen S**, Kamarck T, Mermelstein R. A global measure of perceived stress. *J Health Soc Behav.* 1983; 24(4):385–396.
- Creutz LM**, Kritzer MF. Estrogen receptor-beta immunoreactivity in the midbrain of adult rats: regional, subregional, and cellular localization in the A10, A9, and A8 dopamine cell groups. *J Comp Neurol.* 2002; 446(3):288–300. doi: 10.1002/cne.10207.
- De Bondt T**, Smeets D, Pullens P, Van Hecke W, Jacquemyn Y, Parizel PM. Stability of resting state networks in the female brain during hormonal changes and their relation to premenstrual symptoms. *Brain Res.* 2015; 1624:275–285. doi: 10.1016/j.brainres.2015.07.045.
- Fehring RJ**, Schneider M, Raviele K. Variability in the phases of the menstrual cycle. *J Obstet Gynecol Neonatal Nurs.* 2006; 35(3):376–384. doi: 10.1111/j.1552-6909.2006.00051.x.
- Finn ES**, Shen X, Scheinost D, Rosenberg MD, Huang J, Chun MM, Papademetris X, Constable RT. Functional connectome fingerprinting: Identifying individuals using

- patterns of brain connectivity. *Nat Neurosci.* 2015; 18(11):1664–1671. doi: 10.1038/nn.4135.
- Fornito A**, Harrison BJ, Zalesky A, Simons JS. Competitive and cooperative dynamics of large-scale brain functional networks supporting recollection. *Proc Natl Acad Sci USA.* 2012; 109(31):12788–12793. doi: 10.1073/pnas.1204185109.
- Fox MD**, Greicius M. Clinical applications of resting state functional connectivity. *Front Syst Neurosci.* 2010; 4:19. doi: 10.3389/fnsys.2010.00019.
- Frick KM**, Kim J, Koss WA. Estradiol and hippocampal memory in female and male rodents. *Curr Opin Behav Sci.* 2018; 23:65–74. doi: 10.1016/j.cobeha.2018.03.011.
- Frick KM**, Kim J, Tuscher JJ, Fortress AM. Sex steroid hormones matter for learning and memory: Estrogenic regulation of hippocampal function in male and female rodents. *Learn Mem.* 2015; 22(9):472–493. doi: 10.1101/lm.037267.114.
- Friston KJ**, Rotshtein P, Geng JJ, Sterzer P, Henson RN. A critique of functional localisers. *Neuroimage.* 2006; 30(4):1077–1087. doi: 10.1016/j.neuroimage.2005.08.012.
- Friston KJ**, Williams S, Howard R, Frackowiak RS, Turner R. Movement-related effects in fMRI time-series. *Magn Reson Med.* 1996; 35(3):346–355. doi: 10.1002/mrm.1910350312.
- Galea LAM**, Frick KM, Hampson E, Sohrabji F, Choleris E. Why estrogens matter for behavior and brain health. *Neurosci Biobehav Rev.* 2017; 76:363–379. doi: 10.1016/j.neubiorev.2016.03.024.
- Gibbs SEB**, D’Esposito M. Individual capacity differences predict working memory performance and prefrontal activity following dopamine receptor stimulation. *Cogn Affect Behav Neurosci.* 2005; 5(2):212–221.
- Girard R**, Metereau E, Thomas J, Pugeat M, Qu C, Dreher JC. Hormone therapy at early post-menopause increases cognitive control-related prefrontal activity. *Sci Rep.* 2017; 7:44917. doi: 10.1038/srep44917.

Gordon EM, Laumann TO, Gilmore AW, Newbold DJ, Greene DJ, Berg JJ, Ortega M, Hoyt-Drazen C, Gratton C, Sun H, Hampton JM, Coalson RS, Nguyen AL, McDermott KB, Shimony JS, Snyder AZ, Schlaggar BL, Petersen SE, Nelson SM, Dosenbach NUF. Precision functional mapping of individual human brains. *Neuron*. 2017; 95(4):791–807. doi: 10.1016/j.neuron.2017.07.011.

Granon S, Passetti F, Thomas KL, Dalley JW, Everitt BJ, Robbins TW. Enhanced and impaired attentional performance after infusion of D1 dopaminergic receptor agents into rat prefrontal cortex. *J Neurosci*. 2000; 20(3):1208–1215.

Gratton C, Laumann TO, Nielsen AN, Greene DJ, Gordon EM, Gilmore AW, Nelson SM, Coalson RS, Snyder AZ, Schlaggar BL, Dosenbach NUF, Petersen SE. Functional brain networks are dominated by stable group and individual factors, not cognitive or daily variation. *Neuron*. 2018a; 98(2):439–452. doi: 10.1016/j.neuron.2018.03.035.

Gratton C, Sun H, Petersen SE. Control networks and hubs. *Psychophysiology*. 2018b; 55(3). doi: 10.1111/psyp.13032.

Greicius MD, Flores BH, Menon V, Glover GH, Solvason HB, Kenna H, Reiss AL, Schlaggar AF. Resting-state functional connectivity in major depression: Abnormally increased contributions from subgenual cingulate cortex and thalamus. *Biol Psychiatry*. 2007; 62(5):429–437. doi: 10.1016/j.biopsych.2006.09.020.

Hallquist MN, Hillary FG. Graph theory approaches to functional network organization in brain disorders: A critique for a brave new small-world. *Netw Neurosci*. 2019; 3(1):1–26.

Hampson E, Levy-Cooperman N, Korman JM. Estradiol and mental rotation: Relation to dimensionality, difficulty, or angular disparity? *Horm Behav*. 2014; 65(3):238–248. doi: 10.1016/j.yhbeh.2013.12.016.

Hampson E, Morley EE. Estradiol concentrations and working memory performance in women of reproductive age. *Psychoneuroendocrinology*. 2013; 38(12):2897–2904. doi: 10.1016/j.psyneuen.2013.07.020.

Hao J, Rapp PR, Leffler AE, Leffler SR, Janssen WGM, Lou W, McKay H, Roberts JA, Wearne SL, Hof PR, Morrison JH. Estrogen alters spine number and morphology in prefrontal cortex of aged female rhesus monkeys. *J Neurosci*. 2006; 26(9):2571–2578. doi: 10.1523/JNEUROSCI.3440-05.2006.

Hara Y, Waters EM, McEwen BS, Morrison JH. Estrogen effects on cognitive and synaptic health over the lifecourse. *Physiol Rev*. 2015; 95(3):785–807. doi: 10.1152/physrev.00036.2014.

Hjelmervik H, Hausmann M, Osnes B, Westerhausen R, Specht K. Resting states are resting traits—An fMRI study of sex differences and menstrual cycle effects in resting state cognitive control networks. *PLoS One*. 2014; 9(7):e103492. doi: 10.1371/journal.pone.0103492.

Horien C, Shen X, Scheinost D, Constable RT. The individual functional connectome is unique and stable over months to years. *Neuroimage*. 2019; 189:676–687. doi: 10.1016/j.neuroimage.2019.02.002.

Hyvärinen A, Zhang K, Shimizu S, Hoyer PO. Estimation of a Structural Vector Autoregression Model Using Non-Gaussianity. *Journal of Machine Learning Research*. 2010; 11(56):1709–1731. <http://jmlr.org/papers/v11/hyvarinen10a.html>.

Jacobs E, D’Esposito M. Estrogen shapes dopamine-dependent cognitive processes: Implications for women’s health. *J Neurosci*. 2011; 31(14):5286–5293. doi: 10.1523/JNEUROSCI.6394-10.2011.

Jacobs EG, Holsen LM, Lancaster K, Makris N, Whitfield-Gabrieli S, Remington A, Weiss B, Buka S, Klibanski A, Goldstein JM. 17beta-estradiol differentially regulates stress circuitry activity in healthy and depressed women. *Neuropsychopharmacology*. 2015; 40(3):566–576. doi: 10.1038/npp.2014.203.

Jacobs EG, Weiss B, Makris N, Whitfield-Gabrieli S, Buka SL, Klibanski A, Goldstein JM. Reorganization of functional networks in verbal working memory circuitry in early

midlife: The impact of sex and menopausal status. *Cereb Cortex*. 2016a; 27(5):2857–2870. doi: 10.1093/cercor/bhw127.

Jacobs EG, Weiss BK, Makris N, Whitfield-Gabrieli S, Buka SL, Klibanski A, Goldstein JM. Impact of sex and menopausal status on episodic memory circuitry in early midlife. *J Neurosci*. 2016b; 36(39):10163–10173. doi: 10.1523/JNEUROSCI.0951-16.2016.

Kim J, Frick KM. Distinct effects of estrogen receptor antagonism on object recognition and spatial memory consolidation in ovariectomized mice. *Psychoneuroendocrinology*. 2017; 85:110–114. doi: 10.1016/j.psyneuen.2017.08.013.

Krause DN, Duckles SP, Pelligrino DA. Influence of sex steroid hormones on cerebrovascular function. *J Appl Physiol*. 2006; 101(4):1252–1261. doi: 10.1152/jappphysiol.01095.2005.

Kritzer MF, Creutz LM. Region and sex differences in constituent dopamine neurons and immunoreactivity for intracellular estrogen and androgen receptors in mesocortical projections in rats. *J Neurosci*. 2008; 28(38):9525–9535. doi: 10.1523/JNEUROSCI.2637-08.2008.

Leiva R, Bouchard T, Boehringer H, Abulla S, Ecochard R. Random serum progesterone threshold to confirm ovulation. *Steroids*. 2015; 101:125–129. doi: 10.1016/j.steroids.2015.06.013.

Lisofsky N, Martensson J, Eckert A, Lindenberger U, Gallinat J, Kuhn S. Hippocampal volume and functional connectivity changes during the female menstrual cycle. *Neuroimage*. 2015; 118:154–162. doi: 10.1016/j.neuroimage.2015.06.012.

Mattar MG, Wymbs NF, Bock AS, Aguirre GK, Grafton ST, Bassett DS. Predicting future learning from baseline network architecture. *Neuroimage*. 2018; 172:107–117. doi: 10.1016/j.neuroimage.2018.01.037.

McEwen BS. Redefining neuroendocrinology: Epigenetics of brain-body communication over the life course. *Front Neuroendocrinol*. 2018; 49:8–30. doi: 10.1016/j.yfrne.2017.11.001.

Nebel RA, Aggarwal NT, Barnes LL, Gallagher A, Goldstein JM, Kantarci K, Mallampalli MP, Mormino EC, Scott L, Yu WH, Maki PM, Mielke MM. Understanding the impact of sex and gender in Alzheimer's disease: A call to action. *Alzheimers Dement*. 2018; 14(9):1171–1183. doi: 10.1016/j.jalz.2018.04.008.

Noble S, Spann MN, Tokoglu F, Shen X, Constable RT, Scheinost D. Influences on the test-retest reliability of functional connectivity MRI and its relationship with behavioral utility. *Cerebral Cortex*. 2017; 27(11):5415–5429.

Ohm DT, Bloss EB, Janssen WG, Dietz KC, Wadsworth S, Lou W, Gee NA, Lasley BL, Rapp PR, Morrison JH. Clinically relevant hormone treatments fail to induce spinogenesis in prefrontal cortex of aged female rhesus monkeys. *J Neurosci*. 2012; 32(34):11700–11705. doi: 10.1523/JNEUROSCI.1881-12.2012.

Pasqualini C, Olivier V, Guibert B, Frain O, Leviel V. Acute stimulatory effect of estradiol on striatal dopamine synthesis. *J Neurochem*. 1995; 65(4):1651–1657. doi: 10.1046/j.1471-4159.1995.65041651.x.

Patel AX, Bullmore ET. A wavelet-based estimator of the degrees of freedom in denoised fMRI time series for probabilistic testing of functional connectivity and brain graphs. *Neuroimage*. 2016; 142:14–26. doi: 10.1016/j.neuroimage.2015.04.052.

Petersen N, Kilpatrick LA, Goharзад A, Cahill L. Oral contraceptive pill use and menstrual cycle phase are associated with altered resting state functional connectivity. *Neuroimage*. 2014; 90:24–32. doi: 10.1016/j.neuroimage.2013.12.016.

Plotsky PM, Owens MJ, Nemeroff CB. Psychoneuroendocrinology of depression: hypothalamic-pituitary-adrenal axis. *Psychiatr Clin North Am*. 1998; 21(2):293–307.

Poldrack RA, Laumann TO, Koyejo O, Gregory B, Hover A, Chen MY, Gorgolewski KJ, Luci J, Joo SJ, Boyd RL, Hunicke-Smith S, Simpson ZB, Caven T, Sochat V, Shine JM, Gordon E, Snyder AZ, Adeyemo B, Petersen SE, Glahn DC, et al. Long-term neural and physiological phenotyping of a single human. *Nat Commun*. 2015; 6:8885. doi: 10.1038/ncomms9885.

Pollock V, Cho DW, Reker D, Volavka J. Profile of mood states: the factors and their physiological correlates. *J Nerv Ment Dis.* 1979; 167(10):612–614. doi: 10.1097/00005053-197910000-00004.

Rubinov M, Sporns O. Complex network measures of brain connectivity: Uses and interpretations. *Neuroimage.* 2010 Sep; 52(3):1059–1069. doi: 10.1016/j.neuroimage.2009.10.003.

Rubinow DR, Schmidt PJ. Gonadal steroid regulation of mood: the lessons of premenstrual syndrome. *Front Neuroendocrinol.* 2006; 27(2):210–216. doi: 10.1016/j.yfrne.2006.02.003.

Salehi M, Greene AS, Karbasi A, Shen X, Scheinost D, Constable RT. There is no single functional atlas even for a single individual: Functional parcel definitions change with task. *NeuroImage.* 2020; 208:116366. <http://www.sciencedirect.com/science/article/pii/S1053811919309577>, doi: <https://doi.org/10.1016/j.neuroimage.2019.116366>.

Salehi M, Karbasi A, Barron DS, Scheinost D, Constable RT. Individualized functional networks reconfigure with cognitive state. *Neuroimage.* 2020; 206:116233.

Schaefer A, Kong R, Gordon EM, Laumann TO, Zuo XN, Holmes AJ, Eickhoff SB, Yeo BTT. Local-global parcellation of the human cerebral cortex from intrinsic functional connectivity MRI. *Cereb Cortex.* 2018; 28(9):3095–3114. doi: 10.1093/cercor/bhx179.

Schmidt PJ, Rubinow DR. Sex hormones and mood in the perimenopause. *Ann N Y Acad Sci.* 2009; 1179:70–85. doi: 10.1111/j.1749-6632.2009.04982.x.

Seeley WW, Menon V, Schatzberg AF, Keller J, Glover GH, Kenna H, Reiss AL, Greicius MD. Dissociable intrinsic connectivity networks for salience processing and executive control. *J Neurosci.* 2007; 27(9):2349–2356. doi: 10.1523/JNEUROSCI.5587-06.2007.

Seitzman BA, Gratton C, Laumann TO, Gordon EM, Adeyemo B, Dworetzky A, Kraus BT, Gilmore AW, Berg JJ, Ortega M, Nguyen A, Greene DJ, McDermott KB, Nelson SM, Lessov-Schlaggar CN, Schlaggar BL, Dosenbach NUF, Petersen SE. Trait-like variants in

- human functional brain networks. *Proc Natl Acad Sci USA*. 2019; 116(45):22851–22861. doi: 10.1073/pnas.1902932116.
- Shanmugan S**, Epperson CN. Estrogen and the prefrontal cortex: towards a new understanding of estrogen's effects on executive functions in the menopause transition. *Hum Brain Mapp*. 2014; 35(3):847–865. doi: 10.1002/hbm.22218.
- Sheppard PAS**, Choleris E, Galea LAM. Structural plasticity of the hippocampus in response to estrogens in female rodents. *Mol Brain*. 2019; 12(1):22. doi: 10.1186/s13041-019-0442-7.
- Spielberger CD**, Vagg PR. Psychometric properties of the STAI: A reply to Ramanaiah, Franzen, and Schill. *J Pers Assess*. 1984; 48(1):95–97. doi: 10.1207/s15327752jpa4801{_}16.
- Syan SK**, Minuzzi L, Costescu D, Smith M, Allega OR, Coote M, Hall GBC, Frey BN. Influence of endogenous estradiol, progesterone, allopregnanolone, and dehydroepiandrosterone sulfate on brain resting state functional connectivity across the menstrual cycle. *Fertil Steril*. 2017; 107(5):1246–1255. doi: 10.1016/j.fertnstert.2017.03.021.
- Taylor CM**, Pritchet L, Yu S, Jacobs EG. Applying a women's health lens to the study of the aging brain. *Front Hum Neurosci*. 2019; 13:224. doi: 10.3389/fnhum.2019.00224.
- Thompson TL**, Moss RL. Estrogen regulation of dopamine release in the nucleus accumbens: genomic- and nongenomic-mediated effects. *J Neurochem*. 1994; 62(5):1750–1756. doi: 10.1046/j.1471-4159.1994.62051750.x.
- Van Dijk KR**, Hedden T, Venkataraman A, Evans KC, Lazar SW, Buckner RL. Intrinsic functional connectivity as a tool for human connectomics: Theory, properties, and optimization. *Journal of Neurophysiology*. 2010; 103(1):297–321.
- Vijayraghavan S**, Wang M, Birnbaum SG, Williams GV, Arnsten AFT. Inverted-U dopamine D1 receptor actions on prefrontal neurons engaged in working memory. *Nat Neurosci*. 2007; 10(3):376–384. doi: 10.1038/nn1846.

- Wang ACJ**, Hara Y, Janssen WGM, Rapp PR, Morrison JH. Synaptic estrogen receptor-alpha levels in prefrontal cortex in female rhesus monkeys and their correlation with cognitive performance. *J Neurosci*. 2010; 30(38):12770–12776. doi: 10.1523/JNEUROSCI.3192-10.2010.
- Warren SG**, Juraska JM. Spatial and nonspatial learning across the rat estrous cycle. *Behav Neurosci*. 1997; 111(2):259–266. doi: 10.1037//0735-7044.111.2.259.
- Weis S**, Hodgetts S, Hausmann M. Sex differences and menstrual cycle effects in cognitive and sensory resting state networks. *Brain and cognition*. 2019; 131:66–73.
- Williams GV**, Goldman-Rakic PS. Modulation of memory fields by dopamine D1 receptors in prefrontal cortex. *Nature*. 1995; 376(6541):572–575. doi: 10.1038/376572a0.
- Woolley CS**, McEwen BS. Roles of estradiol and progesterone in regulation of hippocampal dendritic spine density during the estrous cycle in the rat. *J Comp Neurol*. 1993; 336(2):293–306. doi: 10.1002/cne.903360210.
- Yeo BTT**, Krienen FM, Sepulcre J, Sabuncu MR, Lashkari D, Hollinshead M, Roffman JL, Smoller JW, Zollei L, Polimeni JR, Fischl B, Liu H, Buckner RL. The organization of the human cerebral cortex estimated by intrinsic functional connectivity. *J Neurophysiol*. 2011; 106(3):1125–1165. doi: 10.1152/jn.00338.2011.
- Young EA**, Kornstein SG, Harvey AT, Wisniewski SR, Barkin J, Fava M, Trivedi MH, Rush AJ. Influences of hormone-based contraception on depressive symptoms in premenopausal women with major depression. *Psychoneuroendocrinology*. 2007; 32(7):843–853. doi: 10.1016/j.psyneuen.2007.05.013.
- Young EA**, Korszun A. The hypothalamic-pituitary-gonadal axis in mood disorders. *Endocrinol Metab Clin North Am*. 2002; 31(1):63–78.
- Zeydan B**, Tosakulwong N, Schwarz CG, Senjem ML, Gunter JL, Reid RI, Gazzuola Rocca L, Lesnick TG, Smith CY, Bailey KR, Lowe VJ, Roberts RO, Jack CRJ, Petersen RC, Miller VM, Mielke MM, Rocca WA, Kantarci K. Association of bilateral salpingo-oophorectomy

before menopause onset with medial temporal lobe neurodegeneration. *JAMA Neurol.* 2019; 76(1):95–100. doi: 10.1001/jamaneurol.2018.3057.